A preliminary study on the potential of the geothermal resources around the Gulf of Suez, Egypt

Aref Lashin

Abstract The Gulf of Suez is characterized by the presence of many hot springs and deep thermal wells scattered around its coastal areas. So it is considered one of the promised geothermal areas in Egypt. In this study, the main emphasis is to investigate the geothermal potential around the Gulf of Suez using the available logging and geothermometer datasets. The temperature profiles and well logging data of some hot springs and deep wells around or within the coastal area of the Gulf of Suez are used in this study. The temperature profiles are analyzed and some important thermophysical properties are estimated (geothermal gradient, thermal conductivity, heat flow, and specific heat capacity). Such analysis revealed that a medium to high geothermal gradient (22.0–30°C/Km) is given for the Gulf of Suez as a whole, with some spots of much higher gradient in the order of 35.0–44°C/Km (Ras Fanar and Hammam Faraun areas). The compiled thermal plots show that the thick evaporites and rock salt lithology, which is a major constituent in this area, attain the highest thermal conductivity (>3.10 W/m/K) and heat flow (>90 mW/m^2) and the lowest specific heat capacity (<0.30 J/kg/K). The available gamma ray and the natural gamma ray spectroscopy logs are used to conduct a radioactive-based heat generation study using the characteristic radioactive nature of some elements like; ^{238}U, ^{235}U, ^{232}Th, and of the isotope of ^{40}K. A good linearity is observed between the heat production (A in microwatt per cubic meter) and the gamma ray (API) along a wide range of datasets (0–150 API) in all wells. The heat production factor increases in the carbonate lithology (up to $3.20\,\mu W/m^3$) and is proportional to the shale volume. A geothermometer-based study is used to estimate the subsurface formation temperature and heat flow from the geochemical analysis of some water samples collected from the studied hot springs. The estimated thermal parameters are in harmony with the regional thermal regime concluded form logging data. A thermal basin growth study, in relation to the clay diagenesis is conducted concerning the thermal effects that take place with depth giving rise to another clay mineral (illite). Furthermore, a number of 2D thermal–burial history diagrams are constructed for the complied sections of some of the studied areas to show the vertical distribution of the estimated petrothermal properties. A reserve evaluation study is carried out to estimate the economic geothermal capacity of these hot springs to be used as alternative clean source for possible energy production (electricity) and other low-temperature purposes.

Keywords Geothermal resources · Temperature profiles · Heat generation · Geothermometers · Energy production · Gulf of Suez

A. Lashin
Faculty of Science, Geology and Geophysics Department,
King Saud University,
P. O. Box 2455, Riyadh 11451, Saudi Arabia

A. Lashin (✉)
Faculty of Science, Geology Department, Benha University,
P.O. Box 13518, Benha, Egypt
e-mail: aref70@hotmail.com

A. Lashin
Saudi Geological Survey (SGS) Research Chair,
King Saud University,
Riyadh, Saudi Arabia

Introduction

Geothermal field is a geographical definition, it usually indicates an area of geothermal activity at the earth's surface. In cases without surface activity, this term may be used

to indicate the area at the surface corresponding to the geothermal reservoir below (Axelsson and Gunnlaugsson 2000). The geothermal reservoirs can be classified in terms of many parameters, such as their temperature, equilibrium state, and the enthalpy of their fluids. The most important classification is that it takes into account the equilibrium state of the reservoir (Nicholson 1993). It depends mainly on the circulation of the reservoir fluid and the mechanism of heat transfer. In this classification, two geothermal categories can be recognized. The first is the dynamic category, in which the reservoir is continuously recharged by water and discharged into the surface or through the permeable formations. According to the temperature regimes, this category may include high-temperature system ($T > 150$°C) and/or low-temperature system ($T < 150$°C). The second category is the static one that includes normal low-temperature systems and/or geopressured systems, which may be found in large sedimentary basins. Another classification of geothermal reservoirs, which is based on the energy content of the fluids and their potential forms of utilization, classifies the geothermal reservoirs into low, medium, and high enthalpy (or temperature) resources.

The geothermal energy is utilized mainly for electricity production, which is the main engine for the industrial development in a number of countries such as Iceland, New Zealand, Japan, USA, Italy, and Indonesia. The most common non-electric used worldwide (in terms of installed capacity) is heat pumps (34.80%), followed by bathing (26.20%), space heating (21.62%), greenhouses (8.22%), aquaculture (3.93%), and industrial processes (3.13%; Lund and Freeston 2001). The utilization of geothermal energy in developing countries has exhibited an interesting trend over the years. In the 5 years between 1975 and 1979, the geothermal electric capacity installed in these countries increased from 75 to 462 MWe. By the end of the next 5-year period (1980–1984), this figure had reached 1,495 MWe showing a rate of increase during these two periods of 500% and 223%, respectively. In the next 16 years, from 1984 to 2000, there was a further increase of almost 150%. Geothermal power plays a fairly significant role in the energy balance of some areas; for example in 2001, the electric energy produced from geothermal resources represented 27% of the total electricity generated in the Philippines, 12.4% in Kenya, 11.4% in Costa Rica, and 4.3% in El Salvador (Dickson and Fanelli 2004).

In Egypt and the Middle East, the utilization of geothermal energy is still far away from the economic usage. The reasons of this may be argued to many factors such as the low-temperature nature of the encountered geothermal resources in these areas, the presence of other energy sources which are easy to explore and use like rock oil and coal, the lack of the necessary industrial experiences in geothermal utilizations, and the high cost of the energy plants,

which can be constructed for electricity production. However, nowadays, some of the high-quality geothermal plants are constructed for electricity production, in the industrial range, using low boiling point fluids and with low industrial cost. These plants, which are called "Kalina", depend on the ammonia fluid in the engine cycle due to its low boiling point, around 70°C, as compared with the boiling point of water.

The geothermal activity in Egypt is recognized in different areas in terms of small hot springs exposed at the surface or thermal deep wells. Nearly all the hot springs are detected around the coastal parts of the Gulf of Suez and around the Cairo–Suez road (Helwan hot springs). A very good example of the thermal waters, which come from deep wells, are those located in the Western Desert (Kharga and Baharyia oases). Generally, the geothermal resources in Egypt can be categorized as low-temperature potentials and the most important are those located around the Gulf of Suez. In this study, the main emphasis will be on the geothermal activity around the coastal parts of the Gulf of Suez, using available datasets either from the surface shallow hot springs and/or from the deep wells drilled around the Gulf of Suez.

Geothermal activity around the Gulf of Suez

The thermal water activity around the Gulf of Suez can be recognized through a number of hot springs, which can be observed at the surface. Some of these hot springs are detected at the eastern coast of the Gulf of Suez and others are located at the western coast. These springs owe their existence to tectonic (or volcanic) heating associated with the opening of the Red Sea/Gulf of Suez rift (Boulos 1990). The available temperature logs and bottom hole temperature data of some deep oil wells around the coastal areas of the Gulf of Suez are also used as good and direct indicators of the subsurface temperature regimes prevailing in the area.

Hot springs and deep wells

In general, the thermal activity around the Gulf of Suez is controlled by the structural elements affecting the whole gulf area. The major geologic structures affecting the whole province are the NNW–SSE-oriented faults. Figure 1 shows a location map of the different hot springs surrounding the coast of the Gulf of Suez. Some of these hot springs are located in the eastern coast, like Ayun Musa and Hammam Faraun, while others are found in the western coast (Ain El Sukhna). Geologically, Ayun Musa area is generally flat with some minor topographic highs scattered in the area. The stratigraphic column of this area, as inferred from some drilled wells (Ayun Musa 2), is characterized by thick Paleozoic rocks (1,960 ft) unconformably overlying the
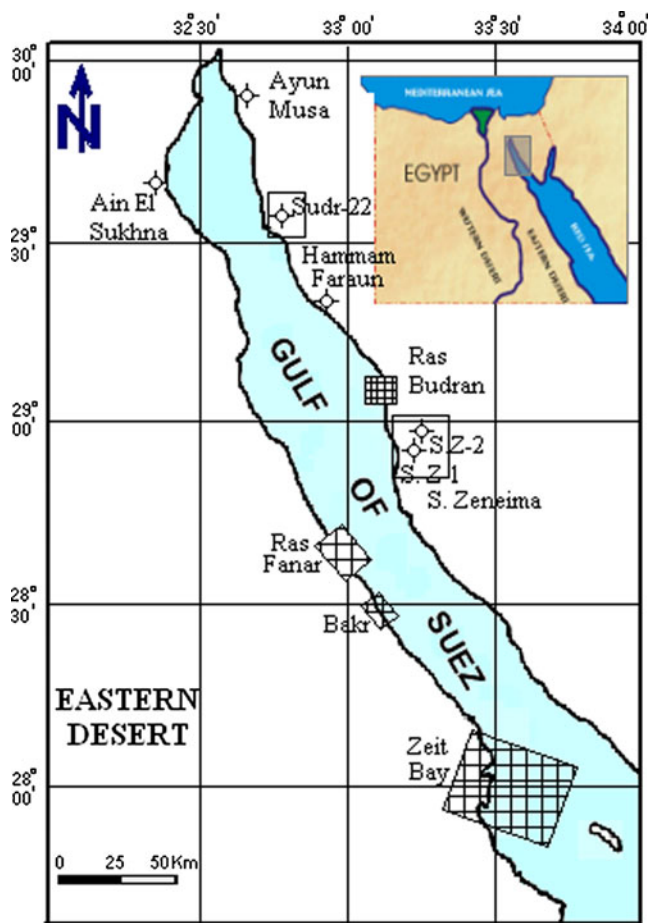
Fig. 1 The Gulf of Suez map showing the locations of the different wells and the hot springs included in this study

Pre-Cambrian basement rocks. The Mesozoic rocks (quartzite, marl, sandstone, and thin limestone beds of about 3,100 ft) are well represented in this area and covered by younger deposits of clays of Miocene age.

Hammam Faraun hot spring is located about 40 km to the south of Sudr area. Due to their proximity, the geologic setting of the Sudr and Hammam Faraun areas is nearly similar. The stratigraphic column is represented by well-classified highly fractured Eocene rocks of considerable thickness (limestone, subordinate shales, marl interbeds, and traces of sandstone), from which the springs flow, covered by thin sediments of the Miocene and Oligocene (gypsum, sandy marl, and conglomerate), and the Pliocene and Post-Pliocene sediments. Ain El Sukhna hot spring, on the other hand, is located in the western coast of the Gulf of Suez. The stratigraphic succession of this area is represented mainly by Miocene deposits of reliable thickness (650 m) overlying a small clastic succession of the Jurassic rocks and underlying a big section consisting of Recent and Post-Miocene deposits.

The available data of deep oil wells scattered along the coastal areas of the Gulf of Suez are used in this study. The stratigraphic successions penetrated by these wells are related to the main geology of the Gulf of Suez, which can be classified stratigraphically into two main groups; the Miocene group (Early: Belayim, South Gharib, Zeit, and Post-Zeit Formations and Middle: Nukhul, Rudies, and Kareem Formations) and the Pre-Miocene group which rests unconformably over the basement rocks. The thick evaporites and rock salt lithology, which is a major rock constituent of the Miocene group, attain the highest thermal properties in the Gulf of Suez area.

Many authors had studied the geothermal activity in Egypt with special emphasis on the Gulf of Suez region. The most important of those are the works of Issar et al. (1971), Morgan and Swanberg (1979), Morgan et al. (1977, 1983, 1985); Swanberg et al. (1983), Riad et al. (1989), Boulus (1989, 1990); Zaghloul et al. (1995), Feinstein et al. (1996), Hosney and Dahroug (1999), Hosney (2000), Hosney and Morgan (2000), Lashin (2007), and Lashin and Al Arifi (2010).

Available data and methodology

This study is based mainly on the temperature profiles and well logging data of some oil fields around or within the coastal area of the Gulf of Suez (±5 km) as well as the geothermometer data acquired from the geochemical analyses of the hot springs. These wells are located both in the eastern (Ayun Musa area, Sudr area, South Zeneima field, and Ras Budran field) and the western (Zeit Bay field and Ras Fanar field) flanks of the Gulf of Suez. The chemical analyses of water samples collected from the hot springs and boreholes (Ayun Musa, Sudr-22, Hammam Faraun, and Ain El Sukhna) are utilized for estimating the subsurface temperature and heat flow.

The study begins with analyzing the temperature data, either as complete temperature runs or as bottom hole temperature guiding points. Horner and Albright methods are used effectively in correcting the bottom hole temperatures and estimating the actual subsurface formation temperature. The geothermal gradient, thermal conductivity, and the regional heat flow around the Gulf of Suez are also estimated. A radioactive-based heat generation study is conducted using the characteristic radioactive nature of some elements like; ^{238}U, ^{235}U, ^{232}Th, and the isotope of ^{40}K. The gamma ray (GR) and the natural gamma ray spectroscopy (NGS) logs are utilized to estimate the rate of radiogenic heat production parameter A in microwatt per cubic meter. Furthermore, the relation between the heat generation (HG) and the acoustic properties of the rocks is investigated.

Geothermometers (silica, Na, K, Ca, etc) are used as indicators to investigate the prevailing subsurface geothermal regimes in the study areas. The ICEBOX software,

which is a mark of the Iceland Geo-survey (ISOR), is used for correcting and estimating the subsurface formation temperature, either from logging data or geochemical analyses. A thermal basin growth study, in relation to the clay diagenesis, is conducted concerning the effect of sedimentation rates and temperature gradients on the transformation cycles of specific clay minerals. With depth and temperature, considerable thermal effects on the acoustic properties of the smectite clay mineral take place, giving rise to another clay mineral (illite), which pertains to different petrothermal characteristics. Furthermore, a number of 2D thermal–burial history diagrams are constructed for some of the study areas around the Gulf of Suez. These diagrams demonstrate the relation between the average basin growth rate (ω) and the increase of thermal burial with depth through the geothermal gradient of the evaluated stratigraphic section. A reserve evaluation study is carried out to estimate the economic geothermal capacity of these hot springs for electricity production purposes and other low-temperature utilizations. Hammam Faraun hot spring is selected, as an example and its geothermal potential is evaluated in terms of the electricity production (thermal megawatt, MW_t).

Analysis and interpretation of temperature data

Estimation of formation temperature

Formation temperature is a very important parameter in the thermal evaluation of any geothermal field. This parameter can be measured directly either as a complete run in boreholes, using a suitable temperature probe, or as separate guiding points at the bottom of each logged interval (bottom hole temperature, BHT). The later procedure is the most commonly used during the logging of deep wells. Most techniques treat temperature as progressive measurements with time after the stop of circulation, to extrapolate the temperature at static conditions (Cheremenski 1960; Jaeger 1961; Edwardson et al. 1962; Schoeppel and Gilarranz 1966; Kehle et al. 1971; Parasnis 1971; Oxburgh et al. 1972; Manetti 1973; Middleton 1979, 1982; Ben Dhia 1988; Kumar 1989; Jones et al. 1989; Lucazeau and Ben Dhia 1989; Correia et al. 1990).

Due to the time difference between the stop of drilling and installing of the logging equipment, some loss in temperature may occur, giving rise to a little bit reduced BHT value than the actual one. In this study, a computer program (BERGHITI, v. 1.3) is used to calculate the actual formation temperature either by the Horner or Albright methods (1975). BERGHITI is a part of the ICEBOX software, which is a copyright of the ISOR and is used mainly for the postdrilling thermal recovery analysis of wells and the calculation of equilibrium rock temperature (Helgason 1993).

Temperature profiles

On studying the geothermal activity within a certain area, a previous knowledge of the prevailing formation temperature in this area is very essential. There are different profiles for the distribution of temperature within the geothermal fields.

Isothermal temperature profiles

Heat transfer dominates by fluid convection; typical profiles are for high permeable geothermal system with temperature that is not too high (T<250°C).

Inverted temperature profiles

Lateral or tilted flow in permeable rock formations. Horizontal and/or tilted fracture flow may also cause inversion of the temperature profiles.

Linear temperature profiles

The linear temperature is dominated in low (vertical) permeability formation. This type is the most common and usually occurs in the low-temperature geothermal fields. Heat transfer dominates by heat conduction and interpretations of temperature are usually carried out through calculating the geothermal gradient, thermal conductivity, and heat flow. Most of the hot springs and geothermal active areas around the coast of the Gulf of Suez are related to this type.
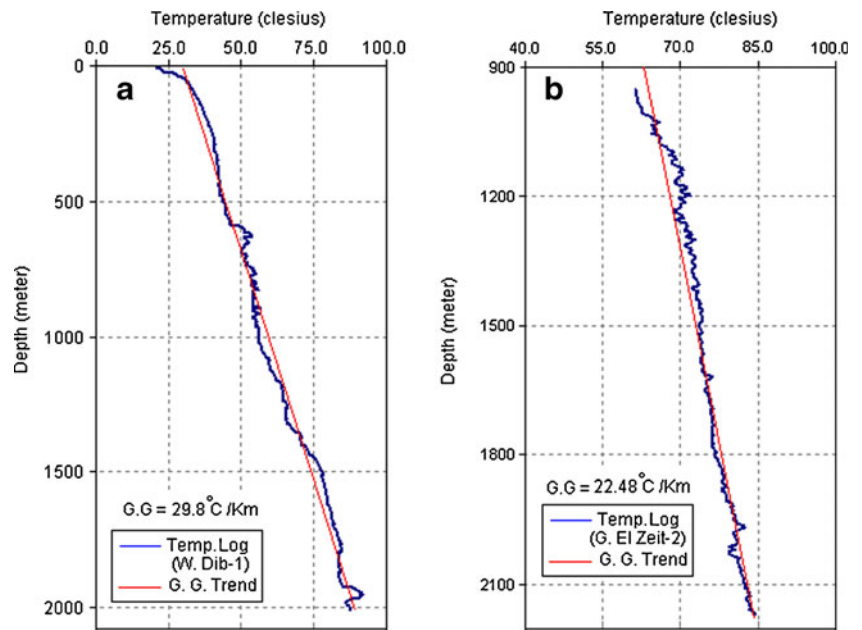
Geothermal gradient

The geothermal gradient is a very important parameter in any geothermal study. The overall heat flow of the earth's surface is generally constant within any particular area; in so doing, the heat flux through the various formations with depth is in equilibrium. The rate of change of temperature across a formation with a low thermal conductivity (due mainly to high porosity) will be high; conversely, a low geothermal gradient is indicative of the high thermal conductivity formations with much lower porosity (Baker Hughes 1996). For a given area, the geothermal gradient, or the rate at which the subsurface temperatures increase with depth is usually assumed to be constant. It can be calculated using the following equation:

$$G.G = \frac{\Delta T}{\Delta Z} = \frac{(T_2 - T_1)}{(Z_2 - Z_1)} \cdot 1000 \tag{1}$$

where, $G.G$ is the geothermal gradient (°C/Km) and ΔT is the temperature change within a depth interval of Z_2–Z_1, (ΔZ in meters).

Figures 2, 3, 4, and 5 show the temperature profiles (logs and BHT) of some selected wells representing the study fields around the coastal parts of the Gulf of Suez. All the temperature profiles exhibit normal linear profiles, only one

Fig. 2 **a** and **b** The temperature logs and the geothermal gradients of W. Dib-1 and G. El-Zeit-2 wells in the Zeit Bay field, Gulf of Suez

exception is found in Hammam Faraun area, where an inverted temperature profile can be clearly observed, indicating the influence of an oriented tilted flow of the geothermal water in this area. The geothermal gradients of the temperature profiles are also indicated in the figures (red solid lines). Medium geothermal gradients are observed in the Zeit Bay and Ras Burdan fields, which range between 22.48–29.8 and 26.1–29.6°C/Km for both fields,

respectively. Meanwhile, the average geothermal gradient in Ras Fanar field tends to be high as it reaches 39.7°C/Km, as seen in Fig. 4. The geothermal gradient of the available
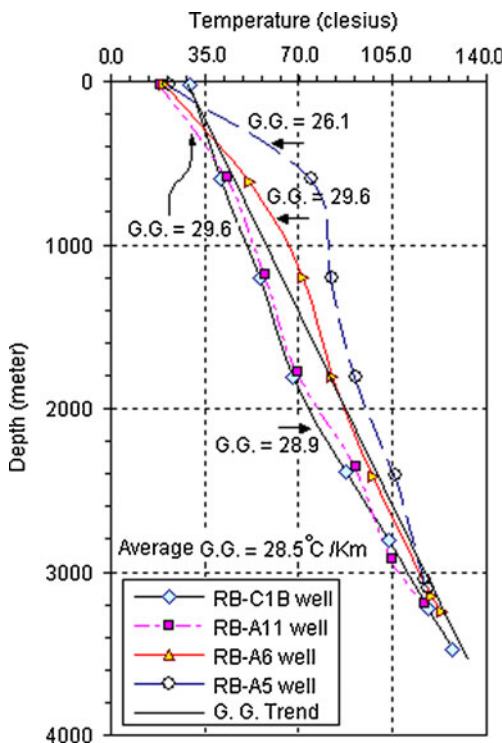

Fig. 3 The temperature profiles and the average geothermal gradient of some wells in Ras Budran field, Gulf of Suez
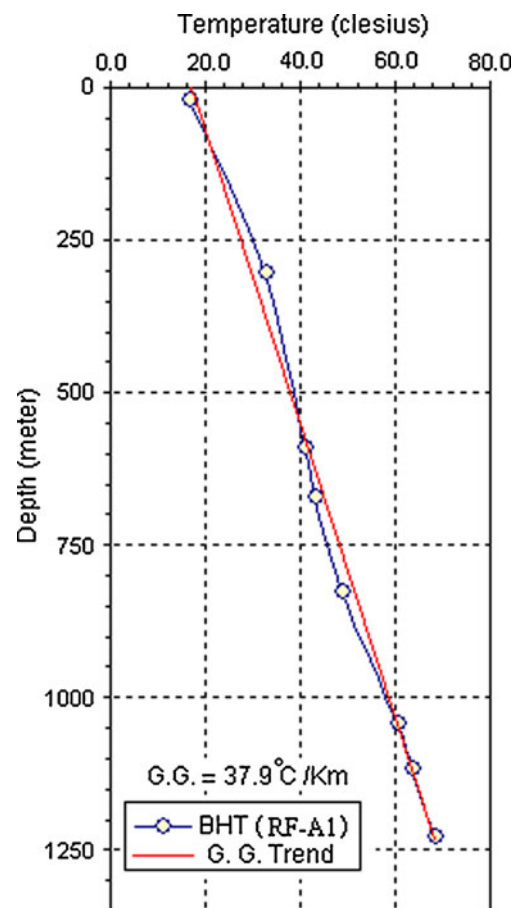

Fig. 4 The temperature profile and the average geothermal gradient of RF-A1 well in Ras Fanar field, Gulf of Suez
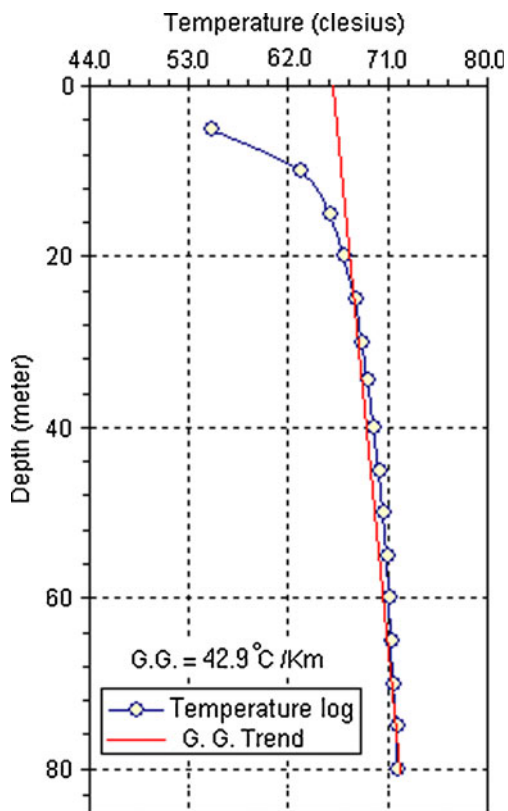
Fig. 5 The temperature log and the average geothermal gradient of a borehole in Hammam Faraun area, Gulf of Suez

temperature data of one borehole in the Hammam Faraun area (Fig. 5) is very high, as it shows a geothermal gradient of 42.9°C/Km. The interpretation of temperature data in the other fields, such as the S. Zeneima field, shows low average geothermal gradient of 19.7°C/Km and much higher gradient in the order of 45.7°C/Km in Bakr oil field.

Thermal conductivity

Thermal conductivity (λ) is a basic physical property of rocks and fluids that changes with rock composition and is inversely proportional to thermal gradient (Prensky 1992). This important thermal petrophysical parameter can be either measured in laboratory using crushed samples and well cuttings or from well logs (Anand et al. 1973; Goss et al. 1975; Hagedorn 1985; Blackwell and Spafford 1987; Beck 1988; Vacquier et al. 1988; Dove and Williams 1989; Brigaud et al. 1989, 1990, 1992; Jessop 1990; Demongodin et al. 1991; Seto and Bharatha 1991; Somerton 1992). Comprehensive compendia of thermal conductivity data are given by Clark (1966), Kappelmeyer and Haenel (1974), and Roy et al. (1981). The in situ thermal conductivity of most sedimentary rocks is in the range of about 1.0–4.5 W/m°C, although some lithologies fall outside of this range. In general, the thermal conductivity of most clastic sedimentary rocks is inversely correlated to their clay content (Deming 1994).

Different types of mixing models have been proposed to relate the thermal conductivity of an aggregate to its individual components. The most common of these is the geometric mean model:

$$\lambda = \lambda_{ma}(1 - \phi) * \lambda_w^\phi \tag{2}$$

where, λ_{ma} is the thermal conductivity of the matrix, λ_w is the thermal conductivity of the pore fluid, and ϕ is the fractional porosity.

Specific heat capacity

Specific heat capacity (joule per kilogram Kelvin; j/kg K) is defined as the amount of heat required to raise the temperature of the unit mass (1 kg) of a substance by a unit temperature increase (1 K). Knowledge of the specific heat capacity is of fundamental importance in geothermal calculations. This parameter is related to the thermal conductivity (λ) and the thermal diffusivity (κ) by the equation:

$$c_p = \frac{\lambda}{\kappa \cdot \rho} \tag{3}$$

where, C_p is the specific heat capacity (J/kg K), κ is the diffusivity and ρ is the density of the rock.

In geothermal fields, in order to calculate the specific heat capacity of water-saturated rocks, the porosity and degree of saturation of the rocks must be known. Because the specific heat capacity of water (C_w) is about five times higher than that of the rock matrix (C_m), the water content of a rock has a dominating influence on the total specific heat capacity (Scharli and Rybach 2001). The following equation can be used:

$$c_{ws} = \frac{c_m \times \rho_m (1 - \phi) + c_w \times \rho_w \times \phi}{\rho_{ws}} \tag{4}$$

where, C_{ws} is the specific heat capacity (J/kg K) and ρ_{ws} is the density of the water-saturated rock.
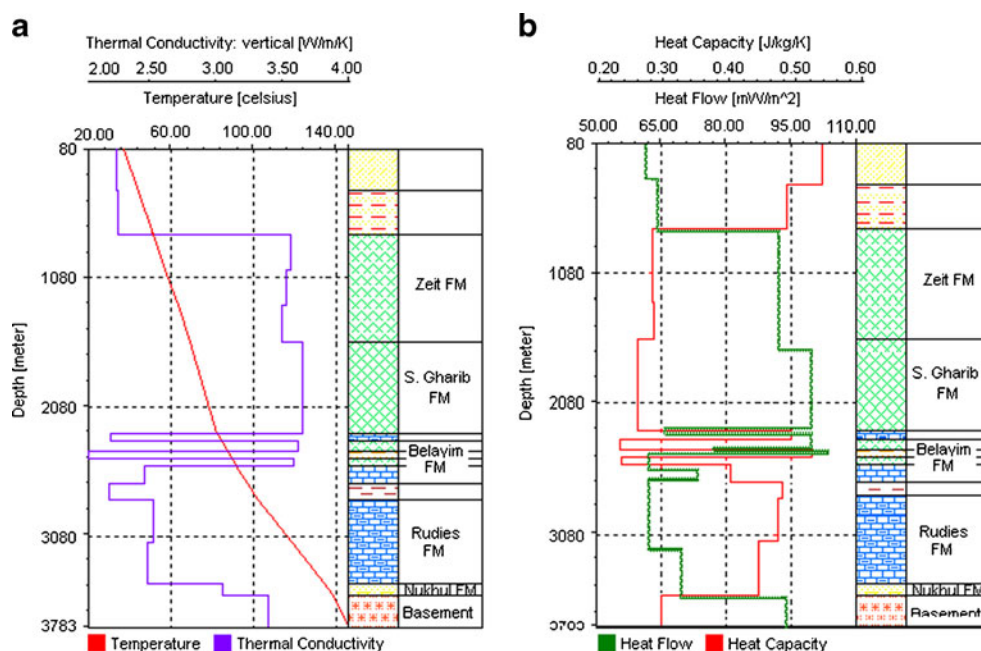
Heat flow

Traditionally, geothermal studies have been concerned with estimating the heat flow, although temperature is the actual quantity of interest. The utility of heat flow studies lies in the ability to infer thermal conditions at great depth from measurements in shallow boreholes (Deming 1994). Heat flow is never measured, but instead is estimated (Eq. 5). If the heat transfer in the crust is by heat conduction alone, then heat flow to the surface is governed by the heat conduction equation, as follows:

$$Q = \lambda \times \Delta T / \Delta Z \tag{5}$$

where, Q is the heat flow (Watt per square meter), T is the formation temperature (degree Celcius), Z is the depth

Fig. 6 **a** The estimated formation temperature and thermal conductivity, **b** Heat flow and heat capacity parameters of Zeit Bay field, Gulf of Suez

(meter), and λ is the thermal conductivity (watt per meter per degree Celcius).

A number of thermal models exhibiting the estimated formation temperature, thermal conductivity, specific heat capacity, and heat flow are constructed for a number of wells and hot springs in certain areas around the Gulf of Suez. Such areas are selected according to the availability of actual temperature logs and/or BHT profiles. For this purpose, the stratigraphic section of each area is compiled from

the geologic sections and the composite logging data of all the available wells in each field.

Figures 6, 7, 8, and 9 represent the constructed thermal diagrams of the Zeit bay, Ras Budran, and Ras Fanar fields, in addition to the Hammam Faraun hot spring. In all figures, the evaporites and rock salt rock units (Zeit and South Gharib Formations and some members in Belayim Formation) along with the basement rocks exhibit the highest estimated thermal conductivity values in watt per meter

Fig. 7 **a** The estimated formation temperature and thermal conductivity, **b** Heat flow and heat capacity parameters of Ras Budran field, Gulf of Suez
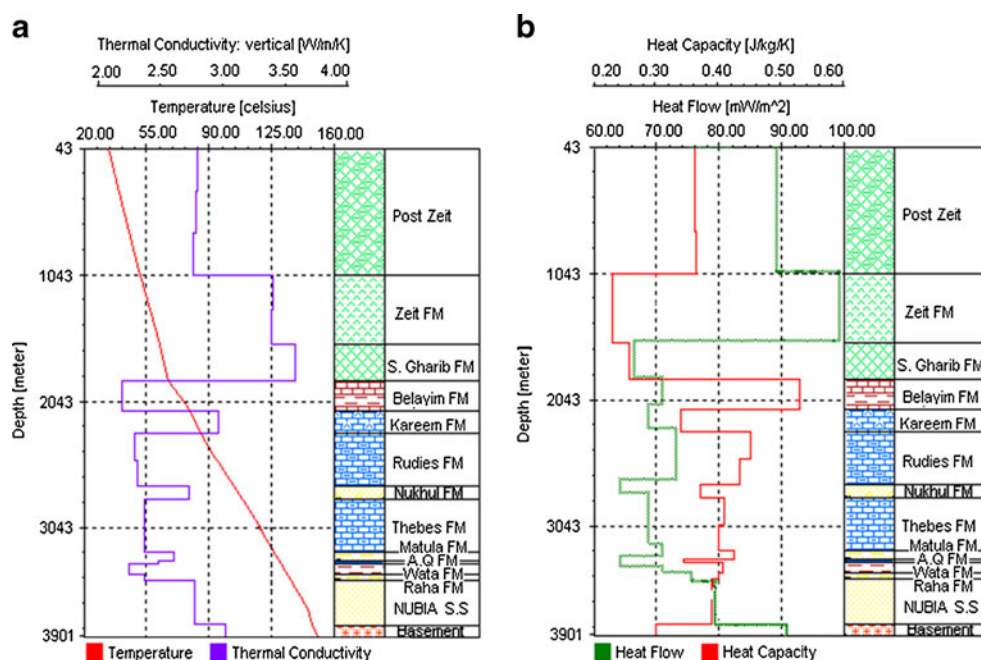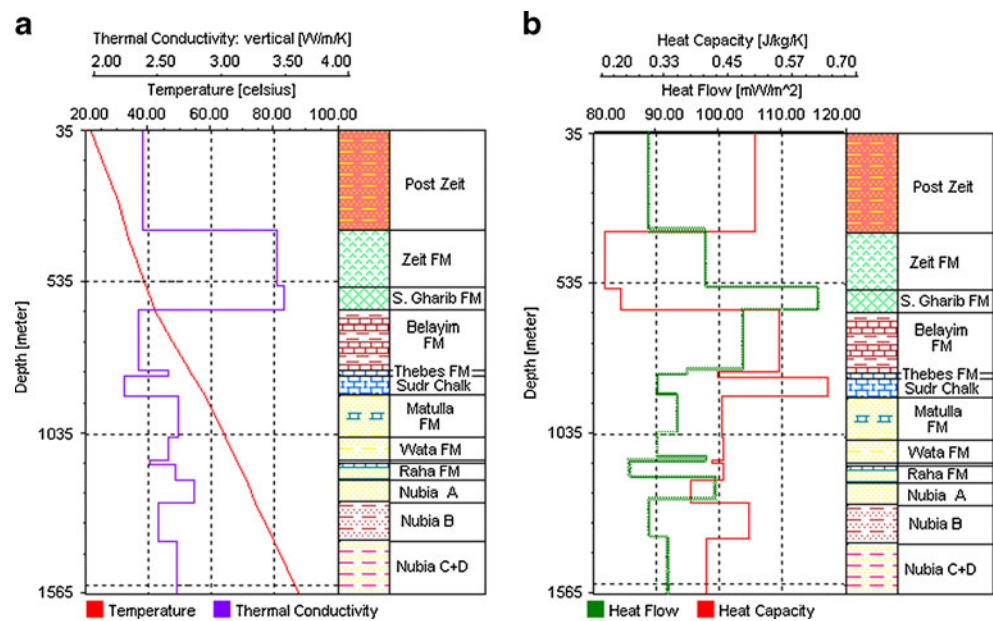
Fig. 8 a The estimated
formation temperature and
thermal conductivity, b heat
flow and heat capacity
parameters of Ras Fanar field,
Gulf of Suez

per Kelvin (3–3.5), the highest heat flow values in milliwatt per square meter (80–100), and the lowest specific heat capacity values (<0.30 J/kg/K). The rock units, where the shale (Watta Formation) and the argillaceous limestone lithology (Thebes Formation) dominate, show low thermal conductivity (<2.5) and heat flow (<65) and high specific heat capacity (>0.50). Some rock units of the Nubia S.S Formation exhibit intermediate petrothermal characteristics.

In Hammam Faraun-Sudr area (Fig. 9), the estimated formation temperature reaches 128°C at a depth of 1,720 m, which is considered high as compared with other comparable depths. Both of the thermal conductivity (2.8–3 W/m/K) and the heat flow (105–120 mW/m^2) increase in front of the U. Eocene rocks suggesting

that these rocks are the possible reservoir of the upcoming geothermal hot water.

Radiogenic heat production

The abundance of the naturally occurring radioactive elements in the earth's crust constitutes a large source of heat supply to the surface heat flow. Therefore, quantifying the vertical and lateral distribution of these elements is of prime interest in any geothermal study. All natural radioactive isotopes generate heat to a certain extent, but only contributions of the decay series of ^{238}U, ^{235}U, ^{232}Th, and of the isotope of ^{40}K are geologically significant. About 40% of the measured heat flux at the earth's

Fig. 9 a The estimated
formation temperature and
thermal conductivity, b heat
flow and heat capacity
parameters of Hammam
Faraun-Sudr area, Gulf of
Suez
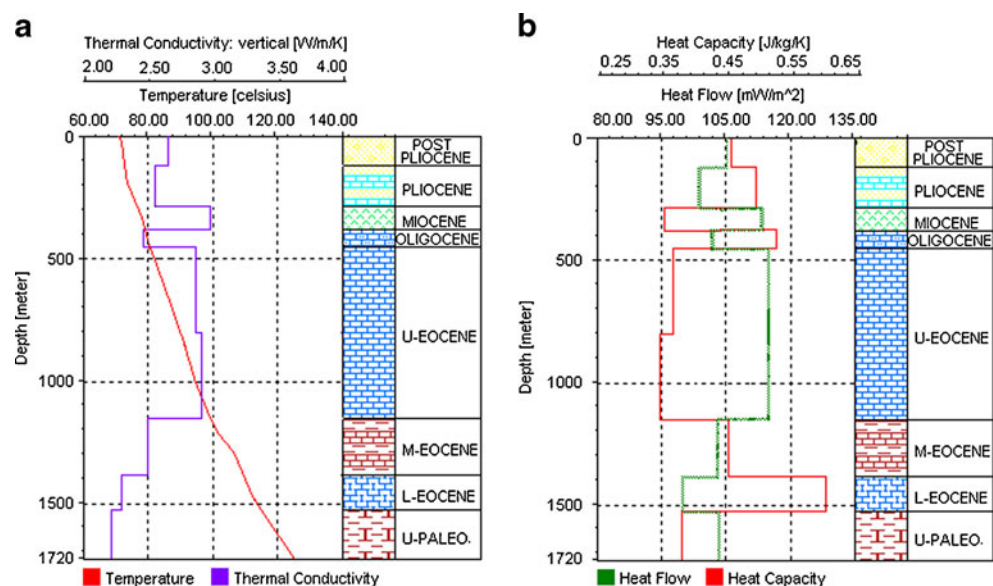
surface on continents comes from the thermal decay of these radioactive elements. The remaining percent (60%) comes from a combination of radioactive sources in the lower crust and upper mantle, as well as a convective flux into the base of the thermal lithosphere (Deming 1994). For studying the geo-thermal potential of a certain area, the concentration of these radioactive elements can be determined analytically when rock samples, either hand specimens or crushed, are available or indirectly using the suitable subsurface logging suites.

In this study, and for some wells around the coastal areas of the Gulf of Suez that have complete logging datasets, the radiogenic heat production can be determined from the integrated gamma ray spectrum or from the natural gamma spectrometry log.

Gamma ray method

The empirical relationship introduced by Buecker and Rybach (1996) is used to derive the heat production from gamma ray readings (API). The general form of this equation is:

$$A\left(\mu W/m^3\right) = a(GR[API] \pm b) \qquad (6)$$

where, A is the rate of radiogenic heat production (microwatt per cubic meter), a and b are empirical constants.

Natural gamma ray spectroscopy

The radiogenic heat production rate (A) is a scalar and isotropic petrophysical property independent of the in situ temperature and pressure. It can be calculated by knowing the concentration of uranium (U), thorium (Th) and potassium (K) elements, and the density (ρ) of the rock (Rybach 1986), according to the following equation:

$$A\left(\mu W/m^3\right) = 10^{-5}\rho(9.52c_U + 2.56_{Th} + 3.48c_K) \qquad (7)$$

where, c_U is the concentration of uranium (parts per million; ppm), c_{Th} is the concentration of thorium (ppm), c_k is the concentration of potassium (percent), and ρ is the rock density (kilogram per cubic meter).

Figures 10, 11, and 12 show the empirical heat production–gamma ray relationships for some wells representing the study fields encountered in the investigated area. It is clear that certain special features are governing the relationship between the two plotted parameters, which are more or less in some wells rather than in the others. Generally, there is a good linearity over the whole gamma ray range from 0 to 150 API in all wells. Two regression lines are indicated (dashed lines), one with high slope for the carbonate dominated lithology and another with low slope for the clastic rocks that have low shale volume. The average regression line (solid line) is indicated between these two slops.

A very good correspondence between the heat production and gamma ray is observed in the Zeit Bay (clastics and carbonates) and S. Zeneima (basement rocks) fields (Figs. 10 and 11). A higher heat production ($A>2.5\,\mu W/m$) is recorded for the carbonate lithology in W. Dib-1 well (Fig. 10a) associated with increasing order of the gamma ray log, while lower response is exhibited by the basement rocks in S. Zeneima field ($A<2.0\,\mu W/m$).

As a whole, the dependence of heat production upon the gamma ray is very good at lower heat production values ($A>0.9\,\mu W/m^3$) as indicated by the narrow scattering of the data-points of the study wells in Ras Budran field (Fig. 12a and b). Meanwhile, at higher heat production, the scattering of data-points relatively increases.

Heat generation and acoustic velocity relationship

In the recent years, many studies have been carried out to examine the relationship between heat generation and acoustic velocity. It is found that heat generation shows a

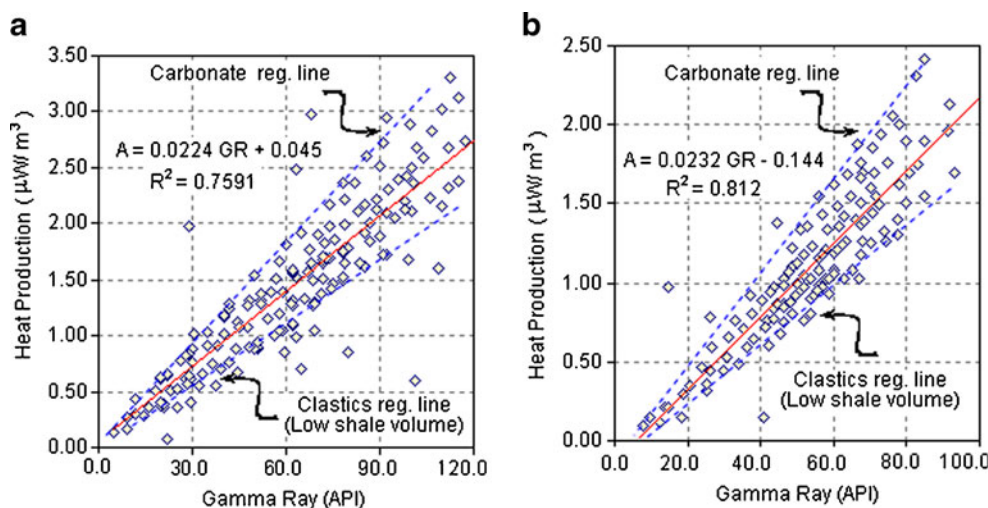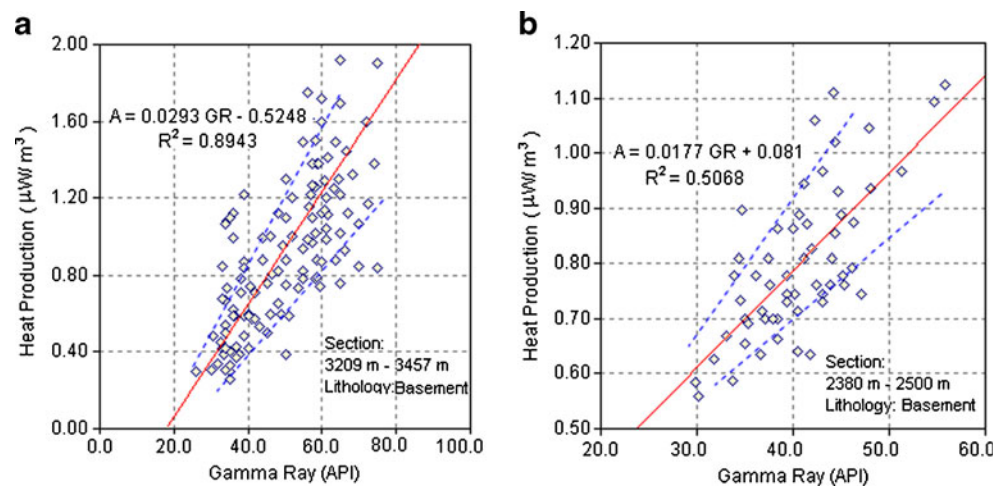Fig. 10 Heat production-gamma ray relationship, a Wadi Dib-1 well and b Gabal El-Zeit-2 well, Zeit Bay field, Gulf of Suez

Fig. 11 Heat production-gamma ray relationship, a S. Zeneima-1 well and b S. Zeneima-2 well, S. Zeneima field, Gulf of Suez

tendency to decrease with increasing the P-wave velocity. Bunterbarth (1975) has found that, for a given pressure and temperature range, there is a systematic variation of the packing index of cations in going from acidic to basic composition of rocks; in turn, the HG decreases and acoustic velocity (V_p) and density increase. On this basis, Rybach (1978) has established the following empirical relationship between heat production and velocity:

$$HG(V_p) = a \exp(-b \cdot V_p) \qquad (8)$$

The numerical constants a and b depend on the depth and pressure of the rock. Figures 13 and 14 show the heat generation–P-wave velocity relationship, where an exponential dependence of heat generation on the V_p is indicated. The uppermost solid lines in the figures indicate the different pressure regimes, which could influence the relationship.

Beyond these lines, the HG–V_p relationship increases at lower pressure, where the effect of fracture and alteration

becomes dominant (Rapolla and Keller 1984). Two examples are selected to demonstrate the constructed relationship between the heat generation and P-wave velocity at different lithology types (hard and soft) around the Gulf of Suez (Figs. 13 and 14). The HG–V_p relationship seems weak for the basement rocks ($R^2 < 11\%$), as represented in Fig. 13.

It appears clear that a pressure regime of the range of 0.50–2.0 kp will influence the HG–V_p relationship over a small range of datapoints in S. Zenemia area (Fig. 13a), while the rest of the other clusters are far from the prevailing pressure regime.

On the one hand, the relationship seems good ($R^2 > 24\%$) for the sedimentary section (Fig. 14), where all the datapoint clusters are located in the area in which the structural control and alteration processes can play a big role. The last relation between the heat generation and P-wave velocity can be further used as a base for exploring the possible subsurface geothermal potential in new areas around the Gulf of Suez, in a regional scale, providing that it is matched with the velocity of a good seismic survey.

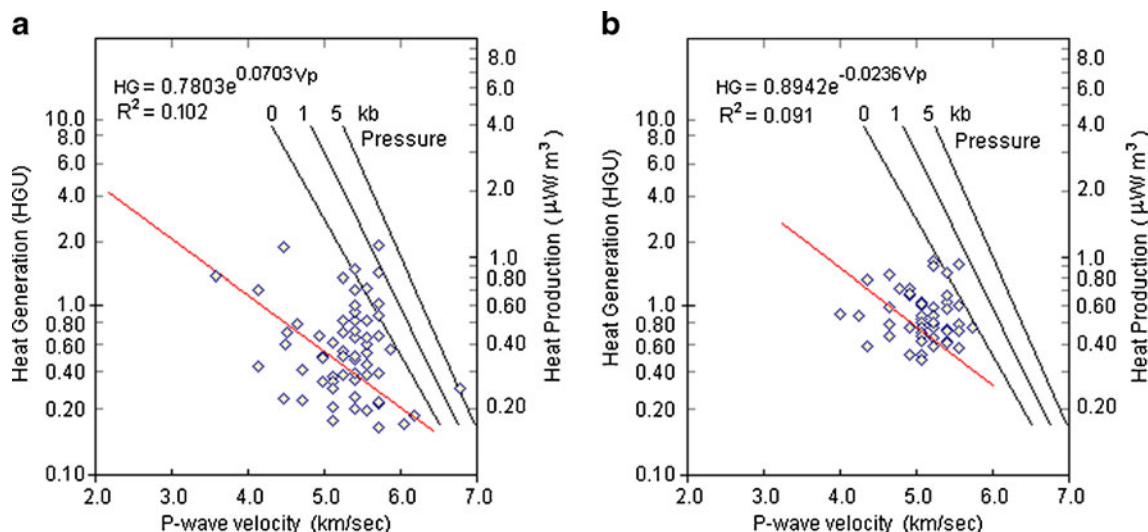Fig. 12 Heat production-gamma ray relationship, a RB-1 well and b RB-A7 well, Ras Budran field, Gulf of Suez
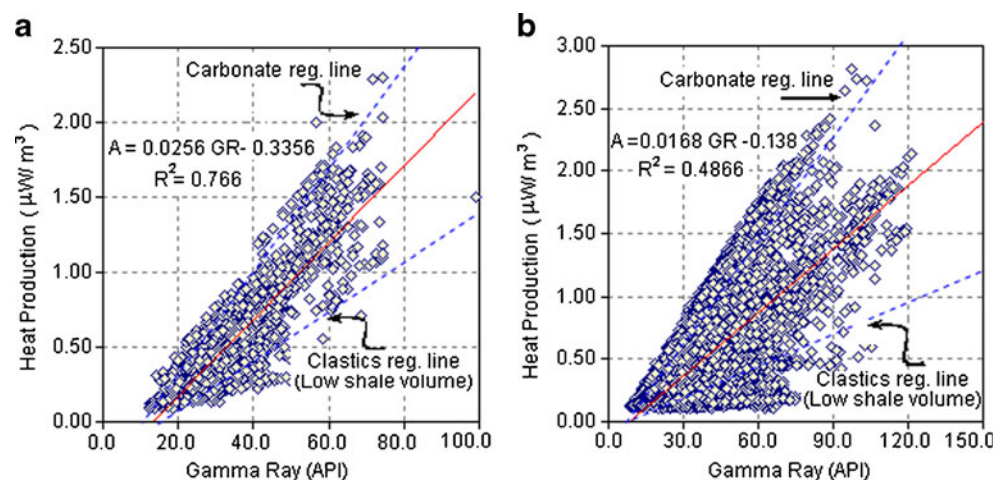
Fig. 13 Heat generation-P wave velocity relationship **a** S. Zeneima-1 well and **b** S. Zeneima-2 well, S. Zeneima field, Gulf of Suez

Geothermometers

Geothermal exploration serves the purpose of locating geo-thermal areas favorable to development and to finding sites within them for drilling. This exploration includes geological mapping, as well as geochemical and geophysical surveys. The principal purpose of geochemical surveys is to predict the subsurface temperatures to obtain information on the origin of the geothermal fluid and to understand the subsurface flow directions. By definition, geothermometer is a chemical sub-stance or isotope in water that may be used to predict the subsurface temperature in geothermal systems. The basic assumption behind using the geothermometers is the chemical equilibrium between the substance (isotope) and mineral (s) in the reservoir. While using these geothermometers, an approximation is made that chemical and isotopic reactions do not significantly modify the composition of the fluid as it ascends from the source aquifer to the point of sam-pling, whether it is at thermal spring, fumaroles, or well-head. Theoretically, any cation ratio and any aqueous species concentration can be used as a geothermometer as long as equilibrium prevails. A temperature equation for a geothermometer is a temperature equation for a specific equilibrium constant referring to a specific mineral-solution reaction (Arnorsson 2000).

Many water geothermometers were developed from the mid-1960s to the mid-2010s. The most important ones are the silica, Na/K, and Na-K-Ca geothermometers. Some other geothermometers are based on the Na/Li, Li/Mg, K/Mg ratios, and Na-K-Mg relationships. Many workers had dealt with
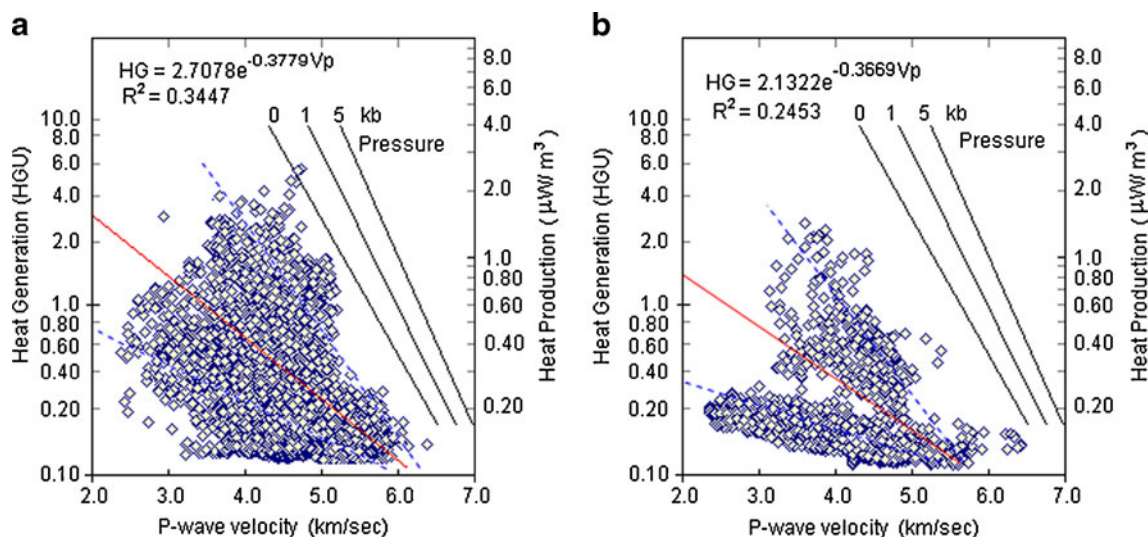

Fig. 14 Heat generation-P wave velocity relationship, **a** RB-A1 well and **b** RB-A7 well, Ras Budran field, Gulf of Suez

using the geothermometers for subsurface formation studies. The most important works are those done by Fournier and Rowe (1966), Ellis and Mahon (1977), Fournier (1977), Fournier and Potter (1982), Swanberg et al. (1983), Arnorsson et al. (1983), Arnorsson (1985), Rimstidt (1997), Arnorsson and Stefansson (1999), Arnorsson et al. (2002), Lashin (2007), and Lashin and Al Arifi (2010, 2011).

Silica geothermometers

Silica geothermometers have been widely used in temperature studies since long time ago. There are several known silica polymorphs in nature. They are quartz, amorphous silica, moganite, tridymite, cristobalite, coesite, and stichovite. Chalcedony is a variety of quartz, being composed of

very fine quartz crystals, so their surface energy contributes to their solubility, which explains why chalcedony is more soluble than quartz. Detailed studies on natural chalcedony grains have shown that they are a mixture of two silica polymorphs, quartz and moganite. The silica phases of interest for geochemical studies of geothermal fluids are quartz, chalcedony, and amorphous silica and probably also moganite. The following are the most important forms of silica geothermometers that are used in this study:

Quartz

$$T_1(^\circ C) = \frac{1,309}{5.19 - \log S} - 273.15 \quad \text{range of } ^\circ C : 25\text{–}250 \tag{9}$$

$$T_2(^\circ C) = \frac{-42.2 + 0.28831\,S - 3.6686 \times 10^{-4}S^2}{+3.1665 \times 10^{-7}S^3 + 77.034\log S} \quad \text{range of } ^\circ C : 25\text{–}900 \tag{10}$$

$$T_3(^\circ C) = \frac{-55.3 + 0.3659\,S - 5.3954 \times 10^{-4}S^2}{+5.5132 \times 10^{-7}S^3 + 74.360\log S} \quad \text{range of } ^\circ C : 0\text{–}350 \tag{11}$$

Chalcedony

$$T_1(^\circ C) = \frac{1,032}{4.69 - \log S} - 273.15 \quad \text{range of } ^\circ C : 25\text{–}250 \tag{12}$$

$$T_2(^\circ C) = \frac{1,112}{4.91 - \log S} - 273.15 \quad \text{range of } ^\circ C : 25\text{–}250 \tag{13}$$

Amorphous Silica

$$T_1(^\circ C) = \frac{731}{4.52 - \text{Log}\,S} - 273.15 \quad \text{range of } ^\circ C : 25\text{–}250 \tag{14}$$

$$T_2(^\circ C) = \frac{-121.6 + 0.2694\,S - 1.8101 \times 10^{-4}S^2}{+7.5221 \times 10^{-8}S^3 + 55.114\log S} \quad \text{range of } ^\circ C : 0\text{–}350 \tag{15}$$

Na-K-Ca Geothermometers

The Na-K-Ca geothermometers are also very important for subsurface formation temperature determination. The main advantage of these geothermometers in comparison with the quartz geothermometer, and especially the Na/K geothermometer is that they do not give high and misleading results for cold and slightly thermal, non-equilibrated waters. The

following are a list of equations, which utilize the three cationic geothermometer (Na-K-Ca) or couples of them (Na-K, K-Mg, K-Ca, Na-Ca, etc):

Na-K

$$T_1(^\circ C) = \frac{933}{0.993 + \log(Na/K)} - 273.15 \quad \text{range of } ^\circ C : 25\text{–}250 \tag{16}$$

K-Mg

$$T_1(°C) = \frac{2,330}{7.35 + \log(K^2/Mg)} - 273.15 \quad \text{for } \log(K^2/Mg) > 1.25$$

(17)

$$T_2(°C) = \frac{1,077}{4.033 + \log(K^2/Mg)} - 273.15 \quad \text{for } \log(K^2/Mg) > 1.25$$

(18)

Na-Ca

$$T_1(°C) = \frac{1,096.7}{3.08 - \log(Na/Ca^{0.5})} - 273.15 \quad (19)$$

K-Ca

$$T_1(°C) = \frac{1,930}{3.861 - \log(K/Ca^{0.5})} - 273.15 \quad (20)$$

Na-K-Ca

$$T_1(°C) = \frac{1,647}{\text{Log}(Na/K) + \beta \log(Ca^{0.5}/Na) + 2.24} - 273.15$$

(21)

In this study, the computer program WATCH 2.1, which is introduced by the Icelandic Water Chemistry Group (ICEBOX software), is used for calculating the subsurface temperature. It serves as a tool for interpreting the chemical composition of the geothermal fluids, although it is also useful for nonthermal waters. The geochemical analysis of the thermal water of the hot springs and wells around the coastal areas of the Gulf of Suez (Ayun Musa, Hammam Faraun, Sudr area, and Ain El Sukhna), which are used in this study, are taken from the work of Morgan et al. (1983), Swanberg et al. (1988), and El Refaei and Abdallah (2000).

Table 1 exhibits the reliable estimated subsurface temperatures of the hot springs using some of the aforementioned geothermometer indicators along with their associated heat flow values. The table shows that Hammam Faraun area attains the highest recorded subsurface formation temperature (94.86°C) and heat flow (121.67 mW/m^2) values among the other studied areas. These values are in harmony with the average temperature (95°C) and heat flow (116 mW/m^2) values obtained from the analysis of temperature data (Fig. 9) of the U. Eocene reservoir rocks of Hammam Faraun spring (depth of 475–1,150 m). Table 2, on the other hand, shows an example of an output file (Ayun Musa area) of the analyses carried out by WATCH 2.1 software.

Geothermal basin modeling

The geothermal modeling for a certain basin requires information concerning the sedimentation rates, temperature gradients, and chemical reaction constants.

Table 1 The subsurface temperature and heat flow values estimated using the different geothermometer indicators

Area	Geothermometer		Quartz	Chalcedony	Na-K	Na-Ca	Na-K-Ca
Hammam Faraun	Subsurface temperature	T_1	94.48		63.90	108.62	55.48	106.59
		T_2	94.86		65.71	–	–	–
		T_3	80.41		–	–	–	–
		Used	94.86°C					
	Heat flow		121.67 mW/m^2					
Ayun Musa	Subsurface temperature	T_1	75.11		43.51	60.10	50.34	80.35
		T_2	75.52		46.52	–	–	–
		T_3	60.63		–	–	–	–
		Used	75.52°C					
	Heat flow		92.86 mW/m^2					
Ain Sukhna	Subsurface temperature	T_1	63.44		31.37	91.94	63.28	91.99
		T_2	63.65		34.97	–	–	–
		T_3	48.55		–	–	–	–
		Used	63.65°C					
	Heat flow		75.17 mW/m^2					
Sudr	Subsurface temperature	T_1	86.66		55.72	154.14	78.18	112.65
		T_2	87.18		57.99	–	–	–
		T_3	72.48		–	–	–	–
		Used	87.18°C					
	Heat Flow		110.23 mW/m^2					

Table 2 The geochemical analyses and the subsurface formation temperature estimated using WATCH 2.1 software, Ayun Musa area

```
ICELANDIC WATER CHEMISTRY GROUP                                Program WATCH, version 2.1


================================================================================================
                                        Ayun Musa Area

Water sample (mg/kg)             Steam sample

pH/deg.C           7.00/   .0   Gas (volume %)               Reference temperature    deg.C : 48.3   (Measured)
CO2                 .00          CO2             .00
H2S                 .00          H2S             .00          Sampling pressure     bar abs. :  1.0
NH3                 .00          NH3             .00          Discharge enthalpy       kJ/kg : 202.   (Calculated)
B                   .73          H2              .00          Discharge                 kg/s :   .0
SiO2              27.00          O2              .00          Steam fraction at collection  : 0000
Na               556.60          CH4             .00
K                  8.60          N2              .00          Measured temperature     deg.C : 48.3
Mg                66.400
Ca               196.80          Liters gas per kg
F                  1.050         condensate/deg.C  .00/ .0  Condensate (mg/kg)
Cl                  .00                                      pH/deg.C          .00/  .0
SO4                 .00          Total steam (mg/kg)         CO2             .00
Al                 .150          CO2             .00          H2S             .00
Fe                2.980          H2S             .00          NH3             .00
TDS             2844.00          NH3             .00          Na              .00

Ionic strength =   .02763
Ionic balance :   Cations (mol.eq.) = .03982460    Anions (mol.eq.) = .00004496    Difference (%) =199.55


Deep water components (mg/kg)                      Deep steam (mg/kg)          Gas pressures (bar-abs.)

B                  .73          CO2        .00      CO2        .00       CO2        .000E+00
SiO2             27.00          H2S        .00      H2S        .00       H2S        .000E+00
Na              556.60          NH3        .00      NH3        .00       NH3        .000E+00
K                 8.60          H2         .00      H2         .00       H2         .000E+00
Mg               66.400         O2         .00      O2         .00       O2         .000E+00
Ca              196.80          CH4        .00      CH4        .00       CH4        .000E+00
F                 1.050         N2         .00      N2         .00       N2         .000E+00
Cl                 .00                                                   H2O        .113E+00
SO4                .00                                                   Total      .113E+00
Al                .1500
Fe               2.9800
TDS             2844.00         Aquifer steam fraction =   .0000

Ionic strength =    .02763                                         1000/T (Kelvin) =   3.11
Ionic balance :   Cations (mol.eq.) = .03982105    Anions (mol.eq.) = .00005643    Difference (%) =199.43

Oxidation potential (volts) :    Eh H2S= 99.999   Eh CH4= 99.999   Eh H2= 99.999   Eh NH3= 99.999

Chemical geothermometers (degrees C)
Quartz        75.5   (Fournier & Potter, GRC Bulletin, pp. 3-12, Nov. 1982)
Chalcedony    43.5   (Fournier, Geothermics, vol. 5, pp. 41-50, 1977)
Na/K          60.1   (Arnorsson et al., Geochim. Cosmochim. Acta, vol. 47, pp. 567-577, 1983)


Log solubility products of minerals in deep water

                Theor.    Calc.                Theor.    Calc.                Theor.    Calc.
Adularia       -19.766  -19.104   Albite, low  -18.808  -17.059   Analcime    -14.954  -13.711
Anhydrite       -4.947   99.999   Calcite       -8.701   99.999   Chalcedony   -3.315   -3.348
Mg-Chlorite    -83.020  -89.845   Fluorite     -10.749  -11.249   Goethite     -6.487   99.999
Laumontite     -30.342  -26.618   Microcline   -21.563  -19.104   Magnetite   -33.690   99.999
Ca-Montmor.   -102.021  -68.132   K-Montmor.   -50.523  -36.514   Mg-Montmor. -102.857  -68.367
Na-Montmor.    -50.318  -34.468   Muscovite    -25.162  -15.979   Prehnite    -39.386  -39.620
Pyrrhotite    -125.913   99.999   Pyrite      -187.006   99.999   Quartz       -3.652   -3.348
Wairakite      -26.617  -26.618   Wollastonite  12.673    6.921   Zoisite     -38.027  -38.058
```

Thermal basin growth and clay diagenesis

In certain sedimentary basins with mixed clastic deposits, one of the most important evidences of its thermal growth with depth is the recognition that smectite portion of shales undergoes a transformation into another clay type called illite. This transformation is dependent on the temperature and time of cooking and requires the presence of potassium, which is

usually available in the pore waters. Dutta and Hobart (1999) introduced a new procedure for measuring the thermal growth of certain basin using the logging tools and available temperature data. In this method, the transit time was taken as a substitute indicator for the degree of smectite/illite transformation, in addition to utilizing a time–temperature history to quantify the degree to which the transformation had completed. This ideal scientific approach requires that assumptions be made concerning the initial smectite concentrations, burial rates, temperature gradients, and chemical kinetics constants. According to the aforementioned assumption, the rate of basin growth to a certain depth or formation can be calculated using the following term:

$$Z = \omega \cdot t \tag{22}$$

where, Z is the true vertical depth of the formation, ω is the average basin growth rate, and t is the age of the formation.

ω is expressed by the number of feet of sediment per year. It can be a positive number if the rate of accretion is greater than the combination of the rate of subsidence (compaction) and the rate of erosion. As the temperature of sediments increases with depth, it will be possible to relate the rate of growth with temperature in only one term as follows:

$$T = T_s + G \cdot G \times Z \tag{23}$$

where, T is the true formation temperature, T_s is the surface temperature, GG is the geothermal gradient.

Then by substituting Eqs. 22 and 23, then:

$$T = T_s + G \cdot G \times \omega \times t \tag{24}$$

If the average surface temperature slightly changes or remains constant, then it will be possible to relate the rate of basin growth to the rate of temperature increase:

$$\frac{dT}{dt} = G \times \omega \tag{25}$$

Now we can quantify the influence of the temperature on the diagenesis of sediments (clays), where the rate of change in the number of moles of smectite in a sediment is proportional to the number of moles remaining. Furthermore, Arrhenius equation for the rate of a chemical reaction can be assumed to model the transformation of smectite to illite, as follows:

$$\frac{dN}{dt} = -K \times N \text{ and } K = A\,e^{-E/RT} \tag{26}$$

where, N is the number of moles of smectite, t is the time, K is a constant (rate of change), A is a frequency factor, and E is the activation energy.

Equations 26 can be combined as follows:

$$\frac{dN}{dt} = -N\,\mathrm{A}\,\mathrm{e}^{-E/RT} \tag{27}$$

The inflection point in the transformation occurs at the maximum change rate of $(dN/dt)_{max}$ when $[d/dt\,(dN/dt)]=0$. Differentiation of the last equation and substituting in Eq. 25, will lead to:

$$e^{-E/RT} = (E/RA)T^2 G\omega \tag{28}$$

Taking the logarithms of both sides and assuming that the temperature at which the transformation of smectite to illite is T_m, then:

$$E/RT_m = \ln\!\left(ART_m^2/G\,\omega\,E\right) \tag{29}$$

The last equation serves as a base for determining the temperature of maximum smectite to illite transformation (T_m), then it will be possible to determine the depth (Z_m), density (ρ_m), and acoustic time (Δt_m) of the transformation through a certain sonic/density crossplot.

In its simple form, this sonic/density transform can be considered an improvement over the Gardner method. For any depth interval within a certain sedimentary sequence, where smectite is cooked into illite, there will be considerable thermal affects on the acoustic properties of the cooked interval, giving rise to different petrothermal characteristics. In so doing, three different trends can be suggested by the inspection of crossplots of delta t and density data. So, in geothermal fields that have mixed clastic sediments, sonic/density transform can be used to indicate the expected shale diagenesis. Figures 15 and 16 indicate the presence of cooked illite zones (the middle regression line) in Ras Budran and Ras Fanar areas.

2D thermal models

A number of thermal–burial history diagrams are constructed for the same areas whose stratigraphic sections are
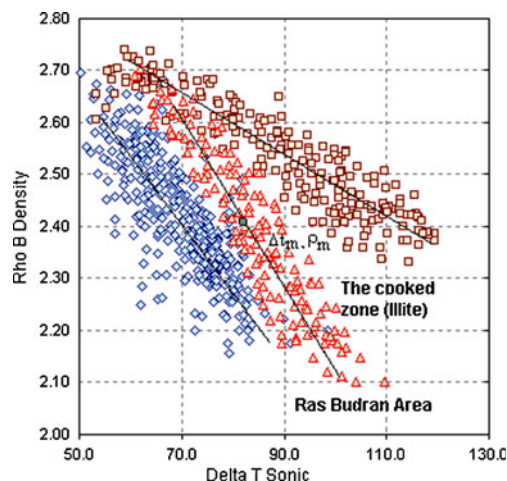

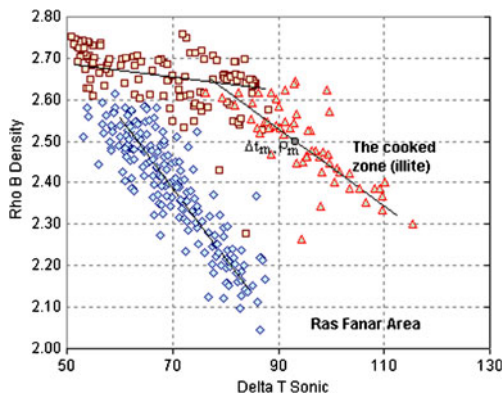Fig. 15 Shale diagenses and the cooked illite zones in Ras Budran field, Gulf of Suez

Fig. 16 Shale diagenses and the cooked illite zones in Ras Fanar field, Gulf of Suez

compiled and used as a model sections, as shown in Figs. 17, 18, 19, and 20. They exhibit the modeled thermal burial history diagrams for the Zeit Bay, Ras Budran, Ras Fanar, and Hammam Faraun areas in a 2D representation. These diagrams illustrate the vertical distribution of the most important thermal parameters (formation temperature, thermal conductivity, heat flow, and heat capacity), taking in consideration the propagated influence of the burial depth and time.

Utilization of geothermal energy

The geothermal resources in Egypt are low-grade energy and can be utilized in terms of low-temperature purposes. In this work, the analyses of the temperature and the geothermometer data show that Hammam Faraun area is the best area to be exploited for geothermal utilization. Both the surface and subsurface thermal waters attain the highest recorded temperature (70°C and 94.5°C, respectively) among the other hot springs encountered along the coastal parts of the Gulf of Suez. The historical and touristic situation of the Hammam Faraun hot spring and its close proximity to the sea-shore are other advantages. In the past, only a few workers had paid their attention to the economic importance of the Hammam Faraun area. The most important work was that of Boulos (1989) and Lashin (2007). Boulos (1989) was first who studied the potentiality of the geothermal resources in an industrial scale. He presented a new idea for applying the ocean thermal energy conversion concept for generating the electricity (150–200 kW) required for tourism development. A single-stage binary plant with ammonia fluid was suggested for this purpose.
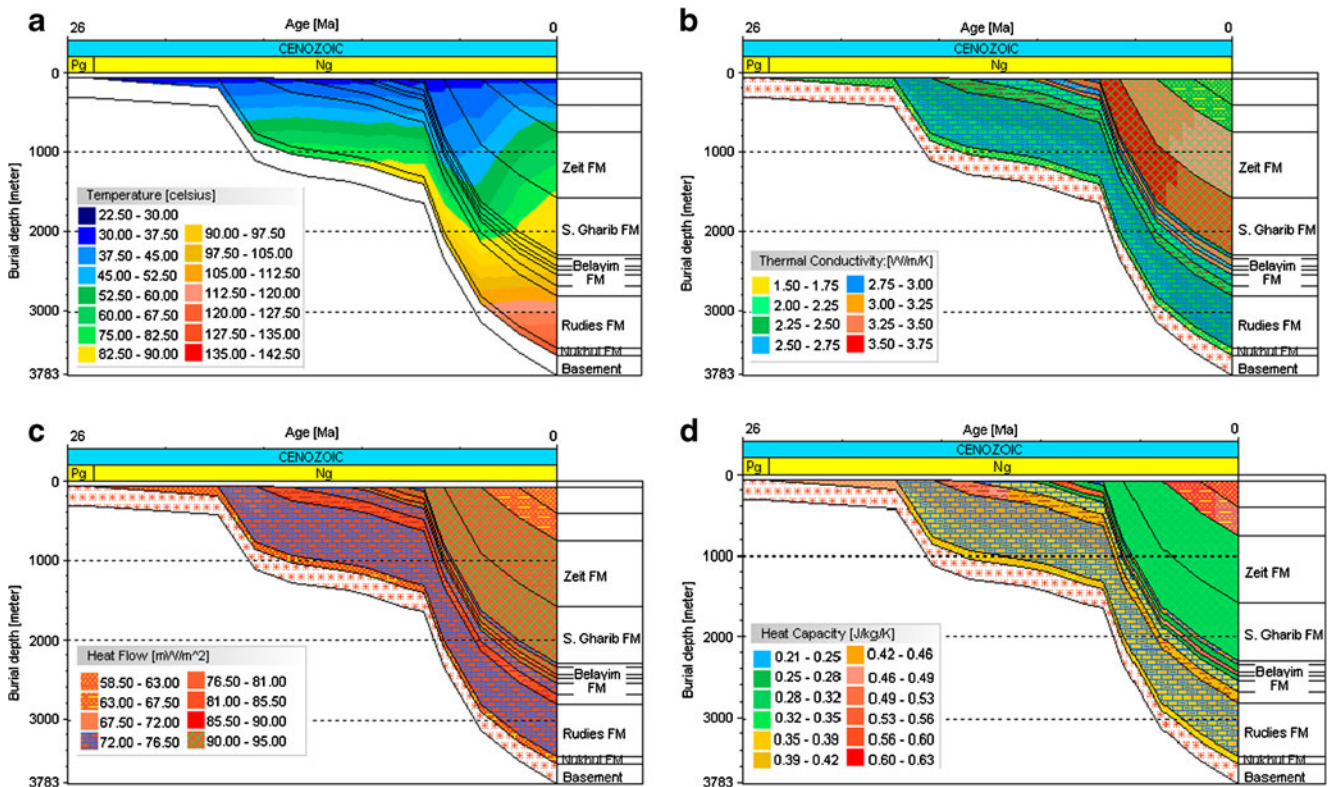

Fig. 17 2D thermal burial history models showing a the formation temperature, b the thermal conductivity, c the heat flow, and d the heat capacity of the Zeit Bay field, Gulf of Suez
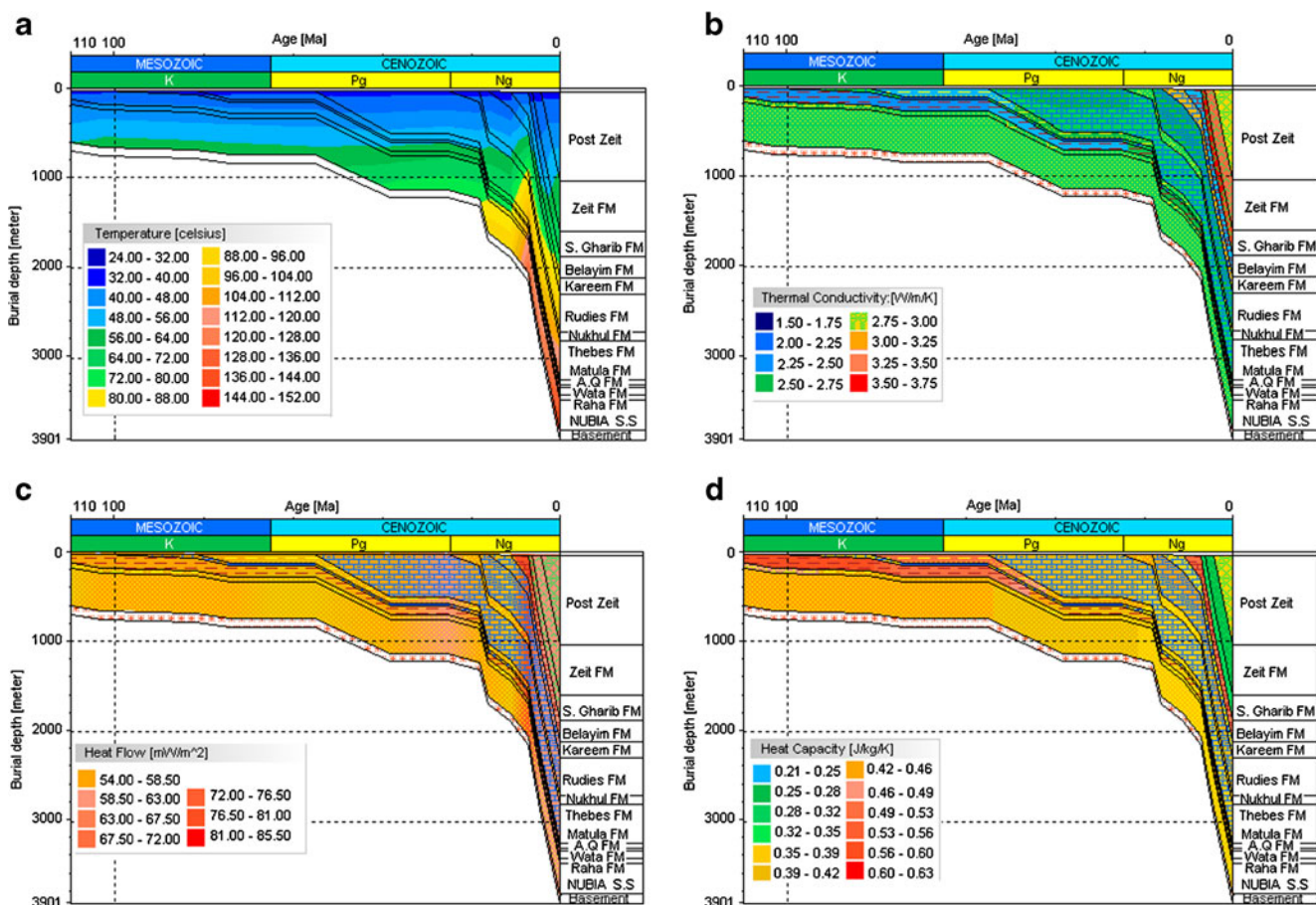
Fig. 18 2D thermal burial history models showing **a** the formation temperature, **b** the thermal conductivity, **c** the heat flow, and **d** the heat capacity of the Ras Budran Field, Gulf of Suez

Geothermal reserve estimation

In this study, a geothermal reserve estimation study is carried out for evaluating the possible geothermal capacities of the geothermal reservoir of Hammam Faraun hot spring. It is selected as an example to check and examine the geothermal potentials of the hot springs around the coastal parts of the Gulf of Suez in an industrial scale for possible electricity production and/or for other low geothermal applications.

The reservoir parameters of the Hammam Faraun hot spring are gathered from the analyses of the temperature data and from other geological information. A computer program (RESPAR, ICEBOX software) is used to estimate the different reservoir properties providing that, the temperature, porosity and the reservoir thickness parameters are known. A reservoir volume of 2.76 km^3 is given for a square area of 2×2 km surrounding the Hammam Faraun hot spring with a provided reservoir thickness of 675 m (thickness of the U. Eocene rocks) and a total depth of 1,150 m (Fig. 9). The initial

temperature of the reservoir is taken as 70°C, while the reference temperature is suggested in this study to be 40°C due to the higher average annual surface temperature in Egypt. Then, the total stored energy of the main fractured limestone reservoir in Hammam Faraun area, which is regarded as the sum of energy stored in the rock (E_r) and the energy represented by the fluid stored in the pore spaces (E_f), can be estimated using the following equation:

$$E_t = E_r + E_f = V(1 - \varphi)\rho_r C_r(T_i - T_o)$$
$$+ V\varphi\,\rho_w C_w(T_i - T_o) \qquad (30)$$

where, E_t is the total thermal energy (Joule) in the rock (E_r) and fluid (E_f), ϕ is the reservoir porosity (percent), V is the reservoir volume (cubic meter), $\rho_{r,w}$ are the densities of rock and water (kilogram per cubic meter), $C_{r,w}$ are the heat capacities of rock and water (Joule per kilogram degree Celcius), and T_i, T_o are the initial reservoir and the reference temperatures (degree Celcius).
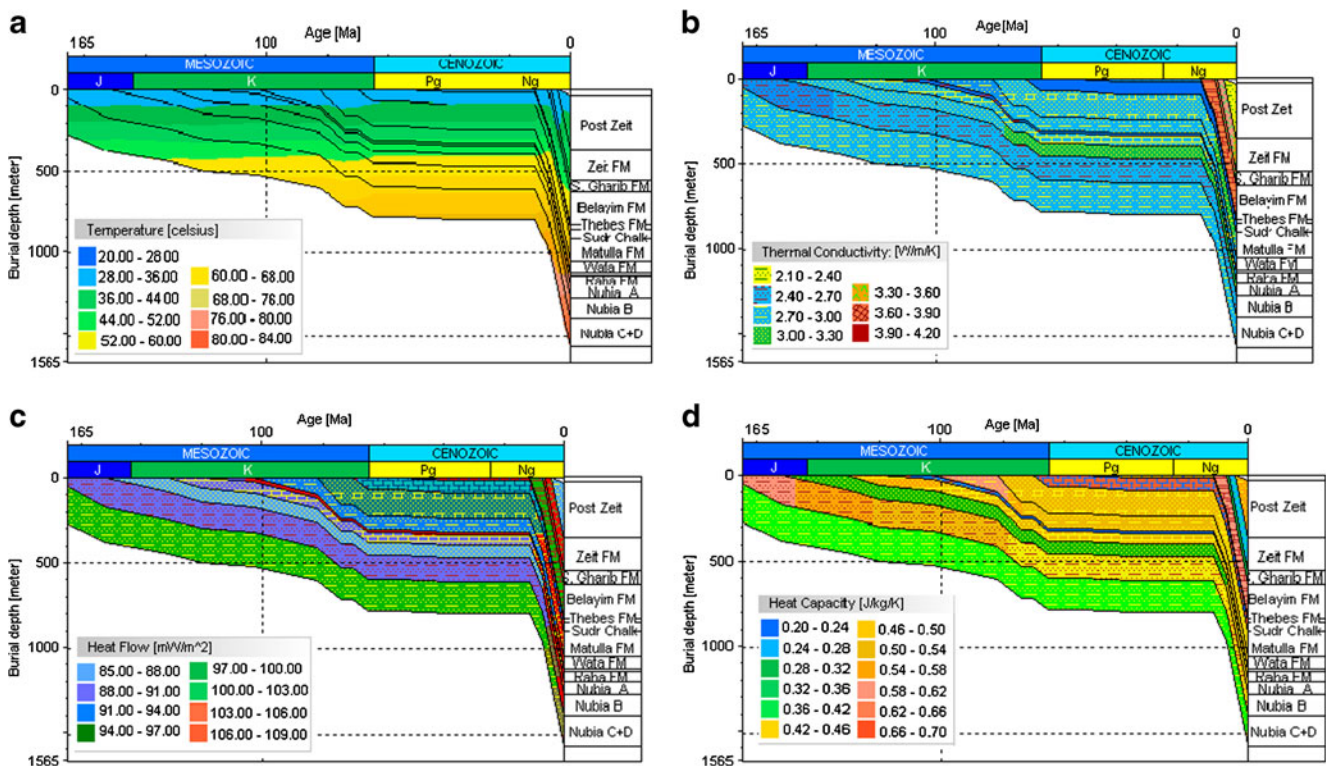
Fig. 19 2D thermal burial history models showing **a** the formation temperature, **b** the thermal conductivity, **c** the heat flow, and **d** the heat capacity of the Ras Fanar field, Gulf of Suez

According to the above equation, the total stored energy in the Hammam Faraun hot spring is calculated to be 2.68×10^{17} J for the reservoir rock and 6.38×10^{16} J for the reservoir fluid. This stored thermal energy can be converted into power potential using the following equation:

$$\text{Power potential}(\text{MWt}) = \frac{E_t \times \text{RF} \times \text{CE}}{\text{PL} \times \text{LF}} \qquad (31)$$

where, RF is the recovery factor, CE is the conversion efficiency, PL is the geothermal plant life in years, and LF is the load factor.

The turbine conversion efficiency factor, which is the ratio between the maximum received temperature of the geothermal reservoir (94.86°C for Hammam Faraun reservoir rocks using downhole pumps) and the actual temperature in the normal home usage (average room temperature in Egypt is 25°C), is found to be 0.26. Supposing that the proposed geothermal plant is assumed to work for 50 years with a recovery factor of 0.20, then the thermal power potential in Hammam Faraun area (Eq. 31) will be 12.4 MW$_t$. The estimated 12.4 MW$_t$ power potential in Hammam Faraun area is economically good and supporting the idea of constructing a small binary power plant for electricity production.

Kalina binary plant

Generating electricity from low-to-medium temperature geothermal fluids (binary plant) and from the waste hot waters coming from the separators in water-dominated geothermal fields has made considerable progress since improvements were made in the binary fluid technology. Binary plant technology is a very effective and reliable mean for converting the energy available from water-dominated (85–170°C) geothermal fields into electricity (Dickson and Fanelli 2004).

The most famous is the Kalina cycle, which was developed in the 1990s and utilizes a water–ammonia mixture as a working fluid. It can be designed in a small-sized mobile plants which, can help in meeting the energy requirements of isolated areas. The convenience of these small mobile plants is most evident for areas and communities, which have no high voltage transmission lines in the vicinity and that would be too expensive to connect to the national electric grid. By selecting suitable secondary fluids and by obtaining the minimum temperature limit, binary systems can be designed to utilize geothermal fluids in the temperature range below 170°C. In Hammam Faraun area, downhole pumps can be used to utilize the downhole thermal waters with temperature more than 85°C. Figure 21 shows a simple design of a small power plant of the Kalina cycle
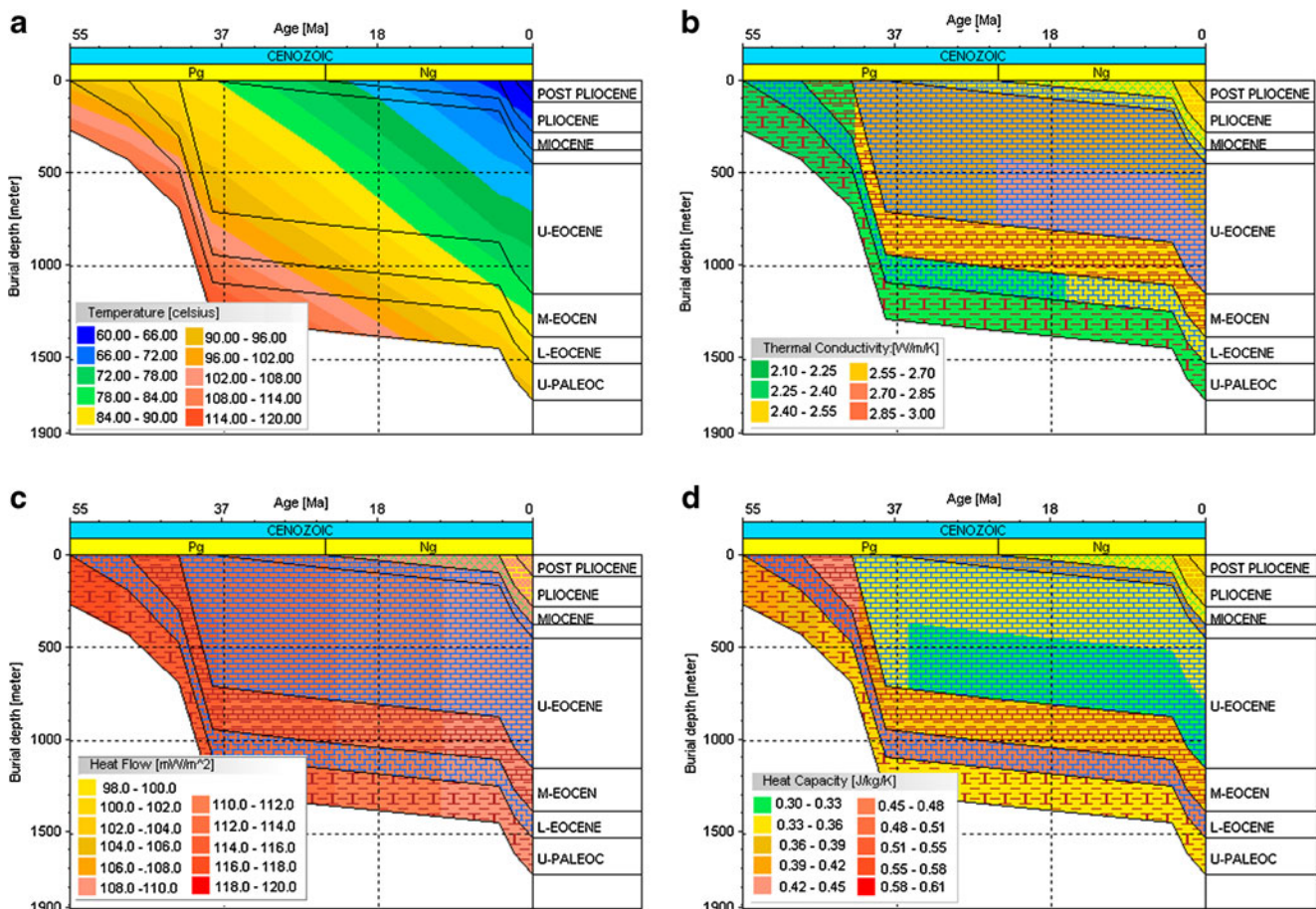
Fig. 20 2D thermal burial history models showing **a** the formation temperature, **b** the thermal conductivity, **c** the heat flow, and **d** the heat capacity of the Hammam Faraun-Sudr area, Gulf of Suez

type, which could be used in Hammam Faraun area (Mannvit 2012). On the other hand, the surface low geothermal water coming from Hammam Faraun can be used for other direct heat applications. The most common forms of utilization are; district heating, fish farming, agricultural applications, and green houses. Constructing a number of swimming pools for touristic purposes is also another important application.

Summary and conclusions

The utilization of geothermal energy in Egypt is still far away from the economic usage. On the last three decades, only few studies have dealt with these resources. The aim of this study is to evaluate the geothermal potentiality around the coastal areas of the Gulf of Suez, using the available logging and geothermometer datasets. The available temperature profiles and well logging data of some oil fields around or within the coastal area of the Gulf of Suez are analyzed and some important thermophysical properties are

estimated (geothermal gradient, thermal conductivity, heat flow, and specific heat capacity). It is found that the geothermal gradient around the Gulf of Suez is generally medium to high (22–30°C/Km). Much higher trends in the order of 35–44°C/Km are observed in some areas (Ras Fanar and Hammam Faraun). The compiled thermal plots show that, the evaporites and the rock salt lithology attains the highest thermal conductivity (>3.10 W/m/K) and heat flow (>90 mW/m^2) as well as the lowest specific heat capacity (<0.30 J/kg/K).

Furthermore, the heat generation factor A (microwatt per cubic meter) is estimated using the gamma ray and the isotopes of ^{238}U, ^{235}U, ^{232}Th, and ^{40}K. A very good correspondence is observed between the heat production and gamma ray especially at lower heat production values ($A >$ 0.9 μW/m^3). The dependence of the HG upon the V_p of the rocks is also investigated. Good HG–V_p relationship is observed beyond the pressure lines indicating that the fractures and alteration are the main controlling factors for the geothermal water. This relationship seems good

Fig. 21 Design of a simple
Kalina power plant (Mannvit
2012)
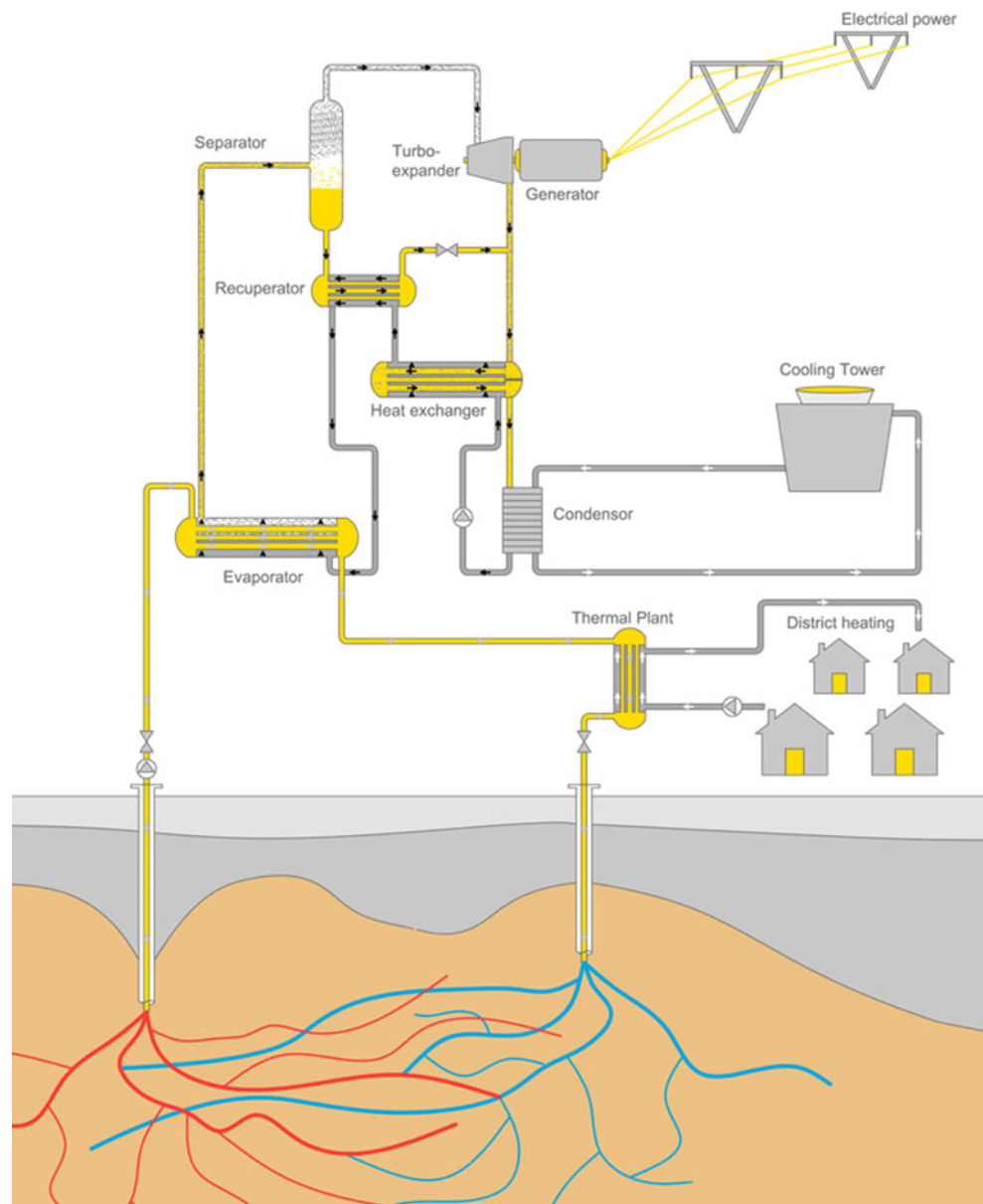
and can be applied in a regional scale for exploring new geothermal targets around the coastal parts of the Gulf of Suez, if it matched with other seismic velocity datasets.

The available geochemical analyses of some hot springs are used for estimating the subsurface formation temperature and heat flow. In this respect, many silica and Na-K-Ca geothermometers are used. The geothermometers show that Hammam Faraun area attains the highest recorded subsurface formation temperature (94.86°C) and heat flow (121.67 mW/m^2) among the other studied areas. These values are in harmony with the comparable values obtained from the analysis of temperature data.

A thermal basin modeling analysis is carried out concerning the petrothermal changes, which some clay minerals (smectite)

undergoes with temperature and depth, giving rise to another mineral (illite). The smectite/illite transformation is recorded in Ras Budran and Ras Fanar fields, where the cooked illite zones are clearly observed in the sonic–density crossplot (the middle regression line). In addition, a number of 2D thermal–burial history diagrams are constructed for the aforementioned estimated petrothermal properties, using the compiled sections of each of the study areas, each alone. The geothermal potential in thermal megawatt is estimated for Hammam Faraun hot spring for electricity production and other low temperature purposes. The estimated geothermal potential is found to be 12.4 MW$_t$, which is considered economic and good for constructing a small binary power plant (Kalina cycle) for electricity production.

Recommendations

The Gulf of Suez is characterized by the presence of some hot springs around its coastal areas. The temperature of the surface geothermal water coming from these springs is not so high, but still accessible for small-scale economic utilization. The present study proved that Hammam Faraun hot spring can produce enough power potential in thermal megawatt to be used in an industrial scale. A binary power plant (Kalina type) is suggested for this purpose. It can be used for limited electricity production and for other low temperature utilization such as; heat pumps, green houses, fish farming, and swimming pools. It is recommended strongly to pay more attention and to increase the scientific work to develop the area around Hammam Faraun spring for touristic purposes on one hand, and for constructing new communities feeded with the geothermal-based energy, on the other hand.

References

Albright JN (1975) A new and more accurate method for direct measurement of earth temperature gradient in deep boreholes. Proc. Sec. U.N. Symposium on the development and use of geothermal resources

Anand J, Somerton WH, Gomaa E (1973) Predicting thermal conductivities of formations from other known properties. Soc Petrol Eng J 13:267–273

Arnorsson S (1985) The use of mixing models and chemical geothermometers for estimating underground temperatures in geothermal systems. J Volcanol Geoth Res 23:299–335

Arnorsson S (2000) Isotopic and chemical techniques in geothermal exploration, development and use: sampling methods, data handling and interpretation. Introductory lecture course, GTP. IS-108, Reykjavik, Iceland, p 199.

Arnorsson S, Stefansson A (1999) Assessment of feldspar solubility constants in water in the range 0 to 350°C at vapour saturation pressures. Am J Sci 299:173–209

Arnorsson E, Gunnlaugsson E, Svavarsson H (1983) The chemistry of thermal waters in Iceland. II. Mineral equilibria and independent variables controlling water compositions. Geochim Cosmochim Acta 47:547–566

Arnorsson S, Gunnarson I, Stefansson A, Andresdottir A, Sveinbjornsdottir AE (2002) Major element chemistry of surface and ground waters in basaltic terrain, N-Iceland. Geochim Cosmochim Acta 66:4015–4046

Axelsson G, Gunnlaugsson E (2000) Background: geothermal utilization, management and monitoring. In: Long-term monitoring of high- and low enthalpy fields under exploitation, WGC 2000 Short Courses, Japan, pp 3–10.

Baker Hughes (1996) Formation pressure evaluation reference guide. Baker Hughes INTEQ Training and Development, Houston, USA, p 292

Beck AE (1988) Methods for determining thermal conductivity and thermal diffusivity, chapter 4.1. In: Haenel R, Rybach L, Stegna L (eds) Handbook of terrestrial heat-flow density determination. Kluwer, Dordrecht, pp 87–124

Ben Dhia H (1988) Tunesian geothermal data from oil wells. Geophysics 53(11):1479–1487

Blackwell DD, Spafford RE (1987) Experimental methods in continental heat flow, chapter 14. In: Sammis CG, Henyey TL (eds) Geophysics, part B, field measurements. Academic, Orlando, FL. Methods of Experimental Physics 24, 189–226.

Boulos F (1989) Geothermal development of Hammam Faraun hot spring, Sinai–Egypt. International conference on applications of solar and renewable energy. p 12

Boulos F (1990) Some aspects of the geophysical regime of Egypt in relation to heat flow, ground water and microearthquakes, chapter, 6. In: Said R (1990) The geology of Egypt. A. A. Balkema, Rotterdam. pp 61–89

Brigaud F, Vasseur G, Caillet G (1989) Use of well log data for predicting detailed in situ thermal conductivity profiles at well sites and estimation of lateral changes in main sedimentary units at basin scale. In: Maury V, Fourmaintraux D (eds) Rock at great depth: A. A. Balkema, Rotterdam, 1, pp 403–409

Brigaud F, Chapman DS, Le Douaran S (1990) Estimating thermal conductivity in sedimentary basins using lithologic data and geophysical well logs. AAPG Bull 74(9):1459–1477

Brigaud F, Vasseur G, Caillet G (1992) Thermal state in the north Viking Graben (North Sea) determined from oil exploration well data. Geophysics 57(1):69–88

Buecker C, Rybach L (1996) A simple method to determine heat generation from gamma ray log. Mar Petrol Geol 13(4):373–375

Bunterbarth G (1975) Geophsilkalische untersuchungen ubes die dissert. Uni. Clausthal

Cheremenski GA (1960) Time of re-establishing the thermal conditions disturbed by drilling a borehole. Bulletin (Izvestiya), Academy of Sciences, USSR, Geophysics Series, no. 12, pp. 1205–1208.

Clark SP Jr (1966) Thermal conductivity. In: Clark SP (ed) Handbook of physical constants: GSA Memoir, p 97.

Correia A, Jones FW, Fricker A (1990) Terrestrial heat-flow density estimates for the Jeanne D'Arc Basin, offshore eastern Canada. Geophysics 55(12):1625–1633

Deming D (1994) Overburden rock, temperature and heat flow. In: Magoon LB, Dow WG (eds) The petroleum system—from source to trap: AAPG Memoir 60, 165–186.

Demongodin L, Pinoteau B, Vasseur G, Gable R (1991) Thermal conductivity and well logs—a case study in the Paris Basin. Geophys J Int 105(3):675–691

Dickson MH, Fanelli M (2004) What is geothermal energy. Internal report. Istituto di Geoscienze e Georisorse, CNR, Pisa, Italy, p 61

Dove RF, Williams CF (1989) Thermal conductivity from elemental concentration logs. Nucl Geophys 3(2):107–112

Dutta N, Hobart S (1999) Pre-drill overburden estimation-1: on the effect of clay diagenesis (smectite to illite) on the density/delta-t crossplot. DEA-119 Project, Report No. 4, Knowledge Systems, Inc., Stafford, Texas, 33–38.

Edwardson MJ, Girner HM, Parkison HR, Williams CD, Matthews CS (1962) Calculation of formation temperature disturbances caused by mud circulation. J Petrol Tech 14(4):416–426

Ellis AL, Mahon WAJ (1977) Chemistry and geothermal systems. Academic Press, New York, p 392

El Refaei AA, Abdallah AM (2000) Hydrogeology of Hammam Faraun Spring, West Central Sinai, Egypt. JMPE 3(1):1–29

Feinstein S, Kohn BP, Steckler MS, Eyal M (1996) Thermal history of the eastern margin of the Gulf of Suez. I. Reconstruction from borehole temperature and organic maturity measurements. Tectonophysics 266:203–220

Fournier RO (1977) Estimating the subsurface formation temperature of the geothermal reservoirs using the soluble chalcedony. Geothermics 5:41–50

Fournier RO, Potter A (1982) Using of quartz geothermometer as indicator for subsurface temperatures. GRC Bulletin, 3–12

Fournier RO, Rowe JJ (1966) estimation of underground temperatures from the silica content of water from hot springs and wet-steam wells. Am J Sci 264:685–697

Goss R, Coombs J, Timur A (1975) Prediction of thermal conductivity in rocks from other physical parameters and from standard geophysical well logs. Paper MM, 16th Annual Logging Symposium Transactions. Society of Professional Well Log Analysts, p 21

Hagedorn DN (1985) The calculation of synthetic thermal conductivity logs from conventional geophysical well logs. Southern Methodist University, unpublished M.S. thesis, p 110

Helgason P (1993) Berghiti, v. 1.3, ICEBOX software. National energy authority of Iceland, Grensasvegi 9, IS-108, Reykjavik, Iceland

Hosney H (2000) Geophysical parameters and crustal temperatures characterizing tectonic and heat flow provinces of Egypt. ICEHM, Cairo Uni., Egypt, 152-166

Hosney HM, Dahroug SM (1999) Nile Delta geothermal data from oil wells. Mansoura Science Bulletin 26(1):49–66

Hosney HM, Morgan P (2000) Geothermal behavior and tectonic setting in the Northern Gulf of Suez, Egypt. J Environ Sci 19:55–74

Issar A, Rosenthal E, Eckstein Y, Bogoch R (1971) Formation waters, hot springs and mineralization phenomena along the eastern shore of the Gulf of Suez. Bull Int Assoc Sci Hydrol 16:25–44

Jaeger JC (1961) The effect of the drilling fluid on temperatures measured in boreholes. J Geophys Res 66(2):563–569

Jessop AM (1990) Thermal geophysics. Dev Solid Earth Geophys 17:306

Jones FW, Majorowicz JA, Embry AF (1989) A heat flow profile across the Sverdrup Basin, Canadian Arctic Islands. Geophysics 54(2):171–180

Kappelmeyer O, Haenel R (1974) Geothermic with special reference to application: Berlin, Gebruder Borntraeger, p 238

Kehle RO, Schoeppel RJ, Deford RK (1971) The AAPG geothermal survey of North America. U.N. symposium on the development and utilization of geothermal resources, Pisa, Italy. Geothermics, special issue 2(1), 358–367

Kumar MB (1989) Geothermal patterns of Louisiana salt domes. Trans Gulf Coast Assoc Geol Soc 29:159–170

Lashin A (2007) Evaluation of the geothermal potential around the coastal parts of the Gulf of Suez, Egypt, using well logging and the geothermometer data. J Appl Geophys 6(2):215–248

Lashin A, Al Arifi NS (2010) Some aspects of the geothermal potential of Egypt. Case study: Gulf of Suez, Egypt. World Geothermal Congress, Bali, Indonesia, p 5

Lashin A, Arifi NS (2011) The Geothermal potential of Saudi Arabia: a case study from the Southwestern parts, Jizan Area. World Renewable Energy Congress, Bali, Indonesia, p 7

Lucazeau F, Ben Dhia H (1989) Preliminary heat-flow density data from Tunesia and the Pelagian Sea. Can J Earth Sci 26(5):993–1000

Lund JW, Freeston D (2001) World-wide direct uses of geothermal energy 2000. Geothermics 30:29–68

Manetti G (1973) Attainment of temperature equilibrium in holes during drilling. Geothermics 2(3/4):94–100

Mannvit (2012) A diagram of the Kalina geothermal power plant in Husavik, Iceland. http://www.mannvit.com/GeothermalEnergy/GeothermalPowerPlants/Kalinacycle-diagram.

Middleton MF (1979) A model for bottom-hole temperature stabilization. Geophysics 44(8):1458–1462

Middleton MF (1982) Bottom-hole temperature stabilization with continued circulation of drilling mud. Geophysics 47(12):1716–1723

Morgan P, Swanberg CA (1979) Heat flow and the geothermal potential of Egypt. Pageoph, V. 117 (1978/1979). Birkhauser, Basel, pp 213–225

Morgan P, Blackwell DD, Farris JC, Boulos FK, Salib PG (1977) Preliminary geothermal gradient and heat flow values for northern Egypt and the Gulf of Suez from oil well data. In: Proceedings, Int. Cong. Thermal Waters: Geothermal Energy and Volcanism of the Mediterranean Area, Nat. Tech. Univ., Athens, Greece, 1, 424–438

Morgan P, Boulos FK, Swanberg CA (1983) Regional geothermal exploration in Egypt. Geophysical Possessing 31:361–376

Morgan P, Boulos FK, Hennin SF, El-Sherif AA, El-Sayed AA, Basta NZ, Mele YS (1985) Heat flow in Eastern Egypt: the thermal signature of a continental breakup. J Geodyn 4:107–131

Nicholson K (1993) Geothermal fluids, XVIII. Springer, Berlin, p 264

Oxburgh ER, Richardson SW, Turcotte DL, Hsui A (1972) Equilibrium borehole temperatures from observation of thermal transients during drilling. Earth Planet Sci Lett 14:47–49

Parasnis DS (1971) Temperature extrapolation to infinite time. Geophys Prospect 19:612–614

Prensky S (1992) Temperature measurements in boreholes: an overview of engineering and scientific applications. Log Analyst 33(3):313–333

Rapolla A, Keller GV (1984) Geophysics of geothermal areas: state of art and future development. Colorado School of Mines Press Pub Centre. Golden, Colorado, 80401, p 306.

Riad S, Abdelrahman E, Refai E, Ghalban H (1989) Geothermal studies in the Nile Delta, Egypt. J Afr Earth Sci 9(314):637–649

Rimstidt JD (1997) Quartz solubility at low temperatures. Geochim Cosmochim Acta 61:2553–2558

Roy RF, Beck AE Jr, Touloukian YS (1981) Thermophysical properties of rocks. In: Touloukian YS, Judd WR, Roy RF (eds) Physical properties of rocks and minerals: McGraw-Hill CINDAS Data Series on material Properties 2(2), 409–502.

Rybach L (1978) The relationship between seismic velocity and radio-active heat production in crustal rocks: an exponential law. Birkauser, Basel, p V117

Rybach L (1986) Amount and significance of radioactive heat sources in sediments. In: Thermal modelling in sedimentary basins, collections. Colloques et Seminaires (Ed J. Burrus) 44, Editions Technio, Paris.

Scharli U, Rybach L (2001) Determination of specific heat capacity on rock fragments. Geothermics 30:93–110

Schoeppel RJ, Gilarranz S (1966) Use of well log temperatures to evaluate regional geothermal gradients. J Petrol Tech 18(6):667–673

Seto AC, Bharatha S (1991) Thermal conductivity estimation from temperature logs. SPE-21542, in SPE International Thermal Operations Symposium Proceedings. Society of Petroleum Engineers 179–186

Somerton WH (1992) Thermal properties and temperature-related behaviour of rock/fluid systems. Dev Petrol Sci 37:250

Swanberg CA, Morgan P, Boulos FK (1983) Geothermal potential of Egypt. Tectonophysics 96:77–94

Swanberg CA, Morgan P, Boulos FK (1988) Geochemistry of the ground waters of Egypt. Ann Geol Surv Egypt 14:127–150

Vacquier V, Mathieu Y, Lengendre E, Blondin E (1988) Experiment on estimating thermal conductivity of sedimentary rocks from oil well logging. AAPG Bull 72(6):758–765

Zaghloul ZM, Shaaban FF, Yousef AF (1995) Subsurface Quaternary geothermal reservoir in the Nile Delta area. J Environ Sci 9:187–204